

Reviewed Preprint

v1 • August 19, 2024

Not revised

Reviewed Preprint

v2 • May 7, 2026

Revised by authors

✉ For correspondence:

[w.zimmermann@med.uni-](mailto:w.zimmermann@med.uni-goettingen.de)[goettingen.de](mailto:w.zimmermann@med.uni-goettingen.de)christoph.schmidt@duke.edu

Competing interests: WHZ is an uncompensated member of the boards of directors of Repairon GmbH and ksilink. WHZ is founder and holds equity of myriamed GmbH and Repairon GmbH. No research funding has been provided by these companies for the reported work.

Funding: See [page 18](#)

Reviewing editor: Pascal Martin, Institut Curie, France

© 2024, Haertter et al. This article is distributed under the terms of the [Creative Commons Attribution License](#), which permits unrestricted use and redistribution provided that the original author and source are credited.

Sarcomere dynamic instability and stochastic heterogeneity drive robust cardiomyocyte contraction

Daniel Haertter^{1,2,3,4,5,6}, Lara Hauke^{1,2,3}, Til Driehorst^{1,5}, Kengo Nishi^{4,5},Wolfram-Hubertus Zimmermann^{1,2,3,6,7} ✉, Christoph F Schmidt^{4,5} ✉

¹Institute of Pharmacology and Toxicology, University Medical Center Göttingen, Göttingen, Germany • ²DZHK (German Center for Cardiovascular Research), Göttingen, Germany • ³CIDAS (Campus Institute Data Science), University of Göttingen, Göttingen, Germany • ⁴Department of Physics and Soft Matter Center, Duke University, Durham, United States • ⁵Third Institute of Physics, Faculty for Physics, University of Göttingen, Göttingen, Germany • ⁶Cluster of Excellence "Multiscale Bioimaging: from Molecular Machines to Networks of Excitable Cells" (MBExC), University of Göttingen, Göttingen, Germany • ⁷Fraunhofer Institute for Translational Medicine and Pharmacology, Göttingen, Germany

eLife Assessment

This **important** study provides a detailed characterization of individual sarcomeres' contractility and of their synchrony in spontaneously beating cardiomyocytes derived from human induced pluripotent stem cells. The combination of high-resolution tracking, statistical analysis and mesoscopic modeling leads to **compelling** evidence that sarcomeres operate as dynamically unstable units, leading to stochastic heterogeneities in their contraction-elongation cycles depending on substrate stiffness. The work will be relevant to scientists interested in muscle biophysics, nonlinear dynamics and synchronization phenomena in biological systems.

<https://doi.org/10.7554/eLife.97321.2.sa4>

Abstract

Cardiac contraction is driven by the collective action of cardiomyocytes, that contain parallel bundles of myofibrils consisting of linear chains of sarcomeres, the basic force-generating units. The dynamics of individual sarcomeres within intact cardiomyocytes remain incompletely understood. While most models assume uniform, synchronized contractions, recent studies hint at unexpected heterogeneity whose origins and significance are not yet clear. By combining the culture of fluorescent sarcomere-reporter hiPSC-derived cardiomyocytes on micropatterned soft gels of different stiffness (5 - 85 kPa) with AI-based tracking of sarcomere motion, we found that increasingly stiff substrates inhibited overall cardiomyocyte contraction, but, surprisingly, did not diminish individual sarcomere dynamics. Instead, sarcomeres competed in a tug-of-war causing increasing heterogeneity, including rapid length oscillations and overextensions (popping). Statistical analysis showed that the heterogeneous dynamics were not caused by static structural differences but were largely stochastic. Stochastic heterogeneity is thus an intrinsic property of cardiac sarcomeres and likely mediates the adaptation of cardiomyocyte contractility to mechanical constraints. A mesoscopic model of coupled sarcomeres shows that these phenomena can be explained by a non-monotonic force-velocity relationship and stochastic fluctuations, where dynamic instability at a critical yielding force creates heterogeneity. Stochastic heterogeneity compensates for structural disorder by randomizing yield events beat-to-beat, preventing damage to specific sarcomeres. Our findings recast cardiac sarcomeres as active, dynamically unstable, and stochastic units engaged in a stochastic tug-of-war, where transient,

velocity-dependent forces dominate. We propose that pathological disorder in cardiomyopathy drives a transition from protective stochastic fluctuations to more deterministic, persistently overloaded sarcomeres.

Introduction

Sarcomeres are the basic contractile cytoskeletal units of striated muscle, including cardiac muscle. In most species, sarcomeres are $\sim 2\ \mu\text{m}$ in length and consist of highly ordered bipolar bundles of myosin motor proteins interdigitated with actin filaments, tied together in the Z-bands. (Fig. 1A). Force generation by myosin interacting with actin is regulated by intracellular Ca^{2+} and fueled by chemical energy (ATP). Sarcomeres are serially connected into myofibrils that span the length of the cell. A cardiomyocyte (CM) contains tens of parallel myofibrils. Overall CM contractility is a mesoscopic process that emerges from a very large number of coupled, non-linear, stochastic, elementary force generators. Despite extensive knowledge of single-molecule motor kinetics and whole-muscle mechanics, this intermediate mesoscopic scale—where tens of sarcomeres interact within a myofibril—remains largely unexplored in cardiac muscle. Sarcomeres are mechanically coupled in series, yet each is also an active, excitable unit undergoing rapid, transient activation-relaxation cycles. Do these coupled sarcomeres maintain synchronized motion, or do stochastic fluctuations and non-equilibrium forces drive heterogeneous behavior?

Recent studies, utilizing in vivo imaging and advanced in vitro models, have begun to reveal notable heterogeneity and beat-to-beat variability at the sarcomere level — even as the average myofibril motion remains smooth and regular. However, these observations have been limited to murine systems ($\approx 5\text{--}8\ \text{Hz}$ beating rate vs. $\sim 1\ \text{Hz}$ in humans). While sarcomere non-uniformity has a long history in skeletal muscle research, prevailing models of cardiac contraction have historically assumed that sarcomeres behave as uniform, synchronized units, with force generation determined primarily by the steady-state force-length relationship—an idea rooted in the Frank-Starling mechanism and length-dependent activation.

Existing attempts to explain cardiac sarcomere heterogeneity remain largely qualitative, invoking static structural differences between sarcomeres—e.g., in strength or resting length—especially pronounced in cardiomyopathy. Such models propose deterministic mechanisms: ‘weak’ sarcomeres are consistently stretched by ‘strong’ neighbors, diastolic length variations dictate subsequent systolic interactions and potential role-switching between sarcomeres, or inherent length variability enables recruitment of more contracting sarcomeres upon cell lengthening through length-dependent activation.

Crucially, these deterministic, primarily length-centric views neglect velocity-dependent active force generation, friction effects, and non-linearities. By assuming a continuous balance between passive and active forces dictated by steady-state relationships, they ignore the non-equilibrium nature of the beating heart, where adaptation kinetics and viscous drag are critical. Consequently, unraveling these dynamics requires novel approaches that resolve the actual motion of individual sarcomeres within their native physiological setting—inside intact, beating cardiomyocytes—tightly integrated with quantitative modeling.

In this study, we cultured human fluorescent sarcomere-reporter hiPSC-derived cardiomyocytes (ACTN2-Citrine-CMs) on micropatterned gel substrates of different stiffnesses to investigate sarcomere dynamics under different mechanical boundary conditions. High-speed imaging, combined with AI-based analysis using our SarcAsM algorithm, enabled us to track average and individual sarcomere motions within myofibrils with nanometer resolution.

Our analysis found strikingly complex dynamic behaviors, including rapid length oscillations, transient ‘popping’ events, and heterogeneous contraction patterns that varied both temporally and spatially along one myofibril. We show that this stochastic heterogeneity appears to arise from competitive, tug-of-war-like interactions among mechanically coupled sarcomeres within the myofibrils. To rationalize these observations, we developed a data-driven mesoscopic model which demonstrates that the emergent heterogeneity at the sarcomere-level can be explained by

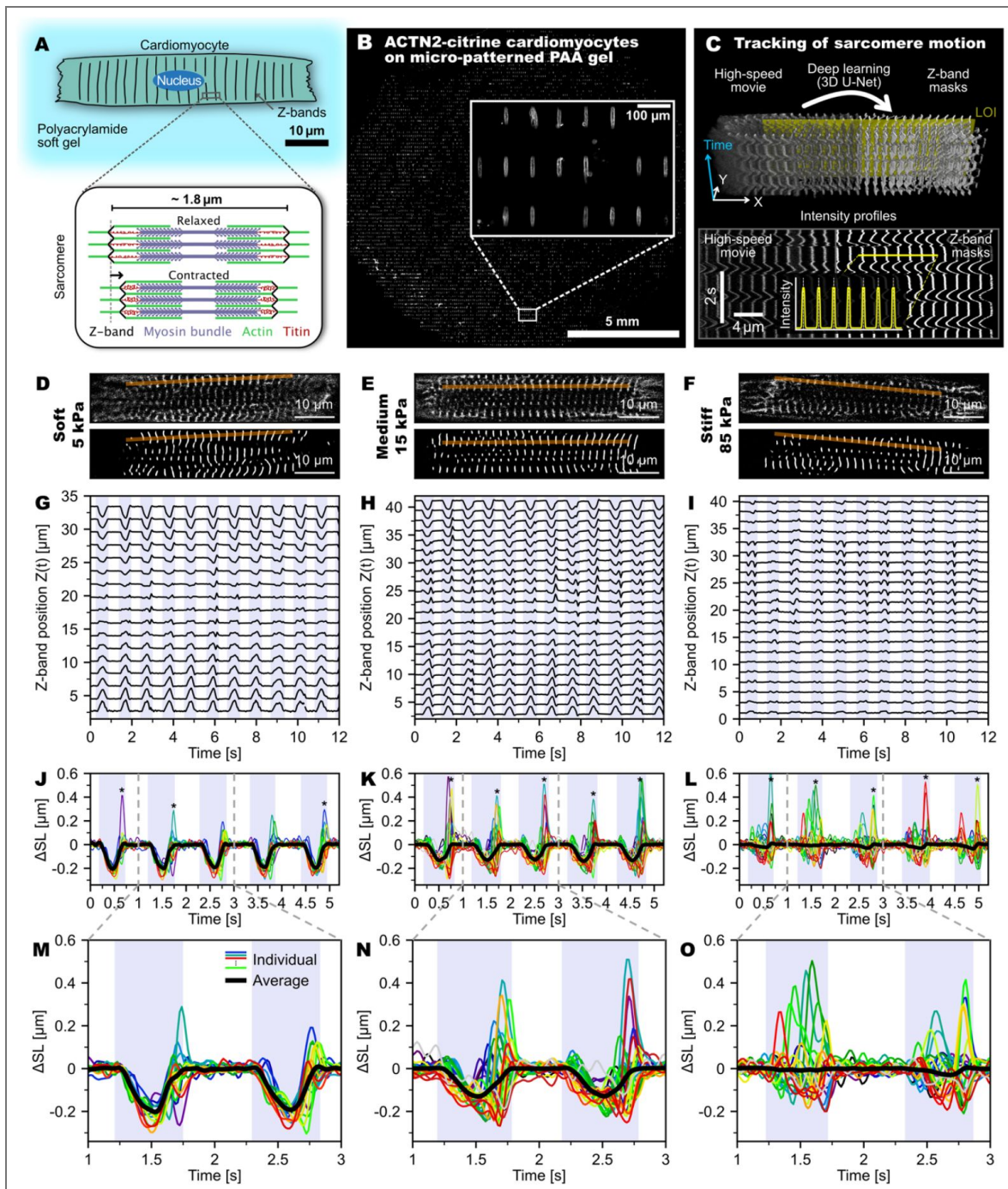


Figure 1. Sarcomere tracking in genetically engineered Z-line labeled iPSC-derived cardiomyocytes on micropatterned soft gels.

(A) Sketch of a human cardiomyocyte (CM) adhering to a micro-patterned gel (top) and sarcomere structure in relaxed and contracted state (bottom). (B) ACTN2-Citrine cardiomyocytes (culture day 20) on a polyacrylamide gel substrate (Young's modulus: 15 kPa), patterned with rectangular stripes of Synthmax (70 × 10 μm). More than 50% of the stripes were typically occupied by single cardiomyocytes. Inset: zoomed-in view. (C) Tracking of sarcomere motion: (Top) blend of high-speed confocal movie of a CM adherent to a 15 kPa substrate (left) and deep-learning (3D U-Net)-based segmentation of sarcomere Z-bands (right) with line of interest (yellow). (Bottom) Intensity extracted along line of interest (LOI). Inset shows representative section of the Z-band intensity profile. (D-E) Confocal images of representative ACTN2-Citrine-labeled CMs with corresponding Z-band segmentation and LOIs (red lines). (G-I) Z-band trajectories tracked along the LOI. (J-L) Overlay plots of single sarcomere length change $\Delta SL(t)$ for all tracked sarcomeres in the marked LOIs (first 5 seconds in J-L, zoomed in M-O). Colored lines are individual sarcomere length changes; black lines display average length changes. Contraction intervals are marked by a blue background. Sarcomere popping events are marked with asterisks. Conditions (substrate stiffness): 5 kPa (D,G,J,M); 15 kPa (physiological): (E,H,K,N); 85 kPa (F,I,L,O).

stochastic fluctuations in conjunction with a non-monotonic force-velocity relation with a critical force threshold. These insights into stochasticity and dynamic instability at the sarcomere level challenge traditional paradigms of myocardial contraction.

Results

Individual ACTN2-Citrine hiPSC-derived CMs on micro-patterned elastic substrates

To resolve sarcomere dynamics with high spatial and temporal resolution in PSC-derived cardiomyocytes, we used a CRISPR-engineered induced pluripotent (iPSC) stem cell line, expressing a yellow fluorescing protein as ACTN2-Citrine N-terminal fusion protein after cardiomyocyte differentiation¹⁵. Seeding of differentiated cardiomyocytes on soft elastic polyacrylamide gels functionalized with a micro-printed pattern ($70 \times 10 \mu\text{m}$; Fig. 1B) promoted anisotropic myofibril assembly in uniformly elongated cardiomyocytes. Culturing cells on gels with defined elasticities (Young's moduli: 5 kPa, 9 kPa, 15 kPa, 29 kPa, 49 kPa, 85 kPa; Table S1) allowed us to impose auxotonic loads on the cells on a scale considered to be relevant *in vivo* under physiological (10-20 kPa) and pathological (e.g., fibrosis; ≥ 30 kPa) conditions¹⁵. After a maturation period of 20-35 days, we recorded 20-30 s long movies of, in total, 1,362 spontaneously beating CMs at a frame rate of 66 Hz (Movie S1, Fig. S1).

Automated tracking of sarcomere motion at high spatial and temporal resolution

We used SarcAsM, an AI-based software tool for automated segmentation and analysis of sarcomere structure and dynamics¹⁵ for data evaluation. SarcAsM automatically identified 5,085 lines of interest (LOIs), up to 4 per cell, with well-organized registered sarcomeres (≥ 10 sarcomeres; Fig. 1C, S1). Along each LOI (~ 800 nm in width), an intensity kymograph of Z-band motion was extracted from deep-learning (3D U-Net) processed movies, allowing for robust and time-consistent segmentation of Z-bands in noisy high-speed movies (Fig. 1C). This approach provided more accurate and robust localization and tracking of Z-band trajectories $Z_i(t)$ of individual sarcomeres than using raw microscopy data (~ 17 nm and 15 ms resolution, details see SarcAsM¹⁵). From $Z_i(t)$, we obtained sarcomere length $SL_i(t)$, sarcomere length change $\Delta SL_i(t)$ and sarcomere velocity $V_i(t)$ of each sarcomere i as well as multi-sarcomere averages $\overline{SL}(t)$, $\overline{\Delta SL}(t)$ and $\overline{V}(t)$ for each LOI (details see SarcAsM¹⁵) (Fig. 1D-F).

Cardiomyocyte and individual sarcomere contractility as a function of substrate stiffness

The hiPSC-CMs were beating spontaneously at a frequency of 0.91 ± 0.38 Hz, which was largely independent of the substrate stiffness (Fig. S2A). Beat-to-beat intervals, though, showed increasing irregularities with increasing substrate stiffness (Fig. S2B). Contraction durations T_c shortened with increasing substrate stiffness (Fig. S2C).

In line with previous reports¹⁶⁻¹⁸, total cell contraction amplitudes, quantified by the inward motion of the outermost z-bands in myofibrils, substantially decreased with increasing substrate stiffness (Fig. 1D-F). A surprising finding was that the length changes of individual sarcomeres ΔSL_i fell out of synchronization and became distinctly heterogenous, deviating strongly from the average length change $\overline{\Delta SL}$ with increasing substrate stiffness. Sarcomeres also showed more singular large-amplitude extensions ("sarcomere popping") far beyond their resting lengths, often very pronounced at the end of contractions (marked with asterisks in bottom row of Fig. 1D-F and large excursions in phase-space plots in Fig. 2A-C). Despite the rapid and heterogenous motion of individual sarcomeres, the emergent contraction at the myofibril scale remained regular and smooth on all substrates.

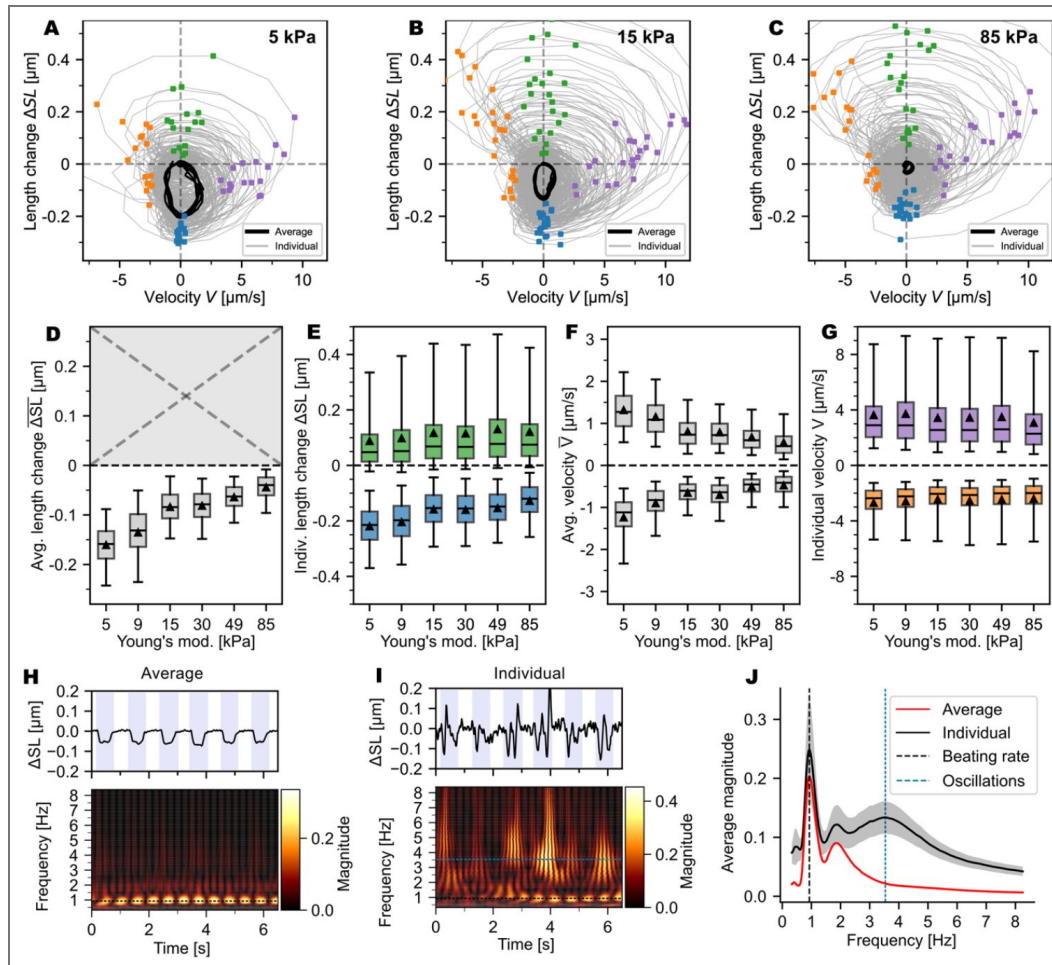


Figure 2. Analysis of sarcomere length change dynamics.

(A-C) Phase-space plots of sarcomere length change ΔSL vs. velocity V for three representative LOIs from CMs on substrates of increasing stiffness (same LOIs as in Fig. 1). Gray lines show individual sarcomere dynamics, black lines average dynamics. Colored dots mark maximal and minimal values of ΔSL and V for individual sarcomere trajectories, with colors corresponding to data in E and G. (D) Box plot of maximal average contractions $\overline{\Delta SL}$ as function of substrate stiffness. Maximal average extensions $\overline{\Delta SL}_+$ are always close to 0 and not shown. (E) Box plot of maximal shortening and lengthening amplitudes $\Delta SL_{+/-}$ of individual sarcomeres quantified in each contraction cycle. (F) Box plot of maximal average sarcomere lengthening and shortening velocities $\overline{V}_{+/-}$. (G) Box plot of maximal individual sarcomere lengthening and shortening velocities $V_{+/-}$. Boxes show quartiles, lines the median, triangles the mean and whiskers the 5th and 95th percentile of the distribution per condition. Each data point corresponds to the extremal value within one contraction cycle. To weigh each LOI equally, only the first 10 contraction cycles in each recording were considered. D-G combine data of 1,652 LOIs (5 kPa: 188, 9 kPa: 586, 15 kPa: 394, 29 kPa: 319, 49 kPa: 506, 85 kPa: 347). Statistical analysis was performed using the Kruskal-Wallis and Dunn's post hoc tests, with significance set at $p < 0.05$. All differences were significant. (H,I) Time series and Morlet wavelet scalogram of average and single sarcomere length changes $\Delta SL(t)$. The top plot displays average (H) and representative single (I) sarcomere length changes over time, with blue background marking contraction periods. The bottom plot presents the wavelet scalograms, depicting the evolution of frequency content in the signal over time, with the blue dashed line signifying the cell's beating rate. (J) Comparison of time-averaged oscillation frequencies of average (red) and single (black) sarcomere length changes of one representative LOI, showing high-frequency intrinsic oscillatory motion of individual sarcomeres with frequencies of 3-4 Hz, which cancel out on the myofibril scale. For time-averaging of the frequency spectra, only the contraction intervals were included. The black curve shows mean \pm S.D. of 16 sarcomeres in one representative LOI; the black dashed line shows the beating rate and the blue dashed line the peak of the oscillation frequency distribution.

To analyze the deviations of individual sarcomere dynamics from the myofibril average during contraction cycles, we collected minima and maxima of ΔSL , i.e., maximal contraction and elongation amplitudes, and minima and maxima of V for each contraction cycle for both individual sarcomeres and averages over all sarcomeres in a given LOI (Fig. 2A-G). In total, we analyzed a data set of 5,085 LOIs recorded from 1,362 cells, each over at least 10 contraction cycles. We excluded irregularly beating (beat-to-beat variability >0.1 s) and very rapidly (>2 Hz) or slowly (<0.5 Hz) beating cells. We further limited the analysis to LOIs spanning whole myofibrils, where the average length change was strictly negative, i.e., showing contraction. Out of the full data set of 5,085 LOIs, 2,321 LOIs met these criteria. This selection ensured that we focused on rhythmically and uniformly contracting cells. As expected, maximal average contraction amplitudes $\overline{\Delta SL}$, measured at the peaks of shortening in each contraction cycle, were the largest ($0.16 \pm 0.05 \mu\text{m}$) on the softest (5 kPa) substrates and were close to zero ($0.04 \pm 0.03 \mu\text{m}$) on the hardest substrates (85 kPa; Fig. 2D). Maximal contraction amplitudes ΔSL_- of individual sarcomeres in each contraction cycle were also largest on 5 kPa substrates at $0.22 \pm 0.09 \mu\text{m}$ and declined to $0.13 \pm 0.07 \mu\text{m}$ on 85 kPa (Fig. 2E). Note that the decline of maximal individual sarcomere shortening (ΔSL_-) by $\sim 30\%$ from 5 to 85 kPa was far less than the $\sim 75\%$ decline of the average sarcomere contraction ($\overline{\Delta SL}$). In addition, while myofibrils never elongated beyond resting length, as expected for auxotonic contractions, individual sarcomeres frequently elongated well beyond their resting lengths during contraction cycles (median $\Delta SL_+ = 0.05 \mu\text{m}$). The distributions of maximal sarcomere extension amplitudes (ΔSL_+) were remarkably similar between substrate conditions (Fig. 2E).

Next, we evaluated the effect of substrate elasticity on average and individual sarcomere contraction and extension velocities. The average extremal velocities \bar{V}_+ and \bar{V} followed the same trend as the extremal average length changes $\overline{\Delta SL}_+$ and $\overline{\Delta SL}$ and were the largest on 5 kPa and declined steadily and strongly with increasing substrate stiffness (from 5 to 85 kPa by $\sim 60\%$ for both contraction and elongation; Fig. 2F). The single sarcomere extremal contraction and extension velocities V_- and V_+ , in contrast, were far less affected by substrate elasticity and differed only by at most $\sim 10\%$ (V_-) and $\sim 20\%$ (V_+) for the various substrate conditions (Fig. 2G). Note that the maximal extension velocities were 29 - 38% larger than the maximal absolute contraction velocities, showing a strong asymmetry between single sarcomere contraction and extension dynamics.

High-frequency oscillatory motion of individual sarcomeres

Unlike the average sarcomere motion with clearly distinguishable contraction and relaxation phases, single sarcomeres exhibited rapid switching between slow contractile and fast extensile motions with sometimes multiple shortening and lengthening phases within one contraction cycle (Fig. 2H,I, Fig. 1D-F). To quantify this phenomenon, we analyzed the oscillation frequencies of the average and individual length changes $\Delta SL(t)$ over time, utilizing Morlet wavelet analysis, a method that makes it possible to extract the instantaneous oscillation frequencies of a signal. For average sarcomere length changes $\overline{\Delta SL}(t)$, the analysis revealed a narrow range of frequencies surrounding the beating rate in the scalogram (Fig. 2H,I). For individual sarcomeres, in contrast, we found a broader range of frequencies, with significant peaks occurring at the dominant and macroscopically visible whole-cell beating rate as well as a large secondary peak at 3 ± 0.5 Hz (Fig. 2J). This distinctive high-frequency oscillation was consistently observed across numerous LOIs and appeared to be independent of the beating rate. The intrinsic oscillatory motion of individual sarcomeres suggests a mechanism of active acto-myosin powered contraction coupled to rapid lengthening in a relaxation oscillator-like behavior¹⁹.

Correlation analysis identifies stochastic and static heterogeneity among sarcomeres

The observed heterogeneity of sarcomere dynamics, particularly on rigid substrates (Fig. 3A), might be predetermined by static non-uniformities among sarcomeres (e.g., by differences in functional myosin numbers). To distinguish this possibility from stochastic heterogeneity, we

extracted the time-resolved motion $\Delta SL_{i,k}(t)$ of each sarcomere i during each contraction cycle k . We then quantified the similarity between these motion patterns using the Pearson correlation coefficient. For two motion patterns $\Delta SL_{i,k}(t)$ and $\Delta SL_{j,l}(t)$, this coefficient is defined as:

$$r(i, j, k, l) = \frac{\sum_{t=1}^T (\Delta SL_{(i,k)}(t) - \overline{\Delta SL_{i,k}}) (\Delta SL_{(j,l)}(t) - \overline{\Delta SL_{j,l}})}{\sqrt{\sum_{t=1}^T (\Delta SL_{(i,k)}(t) - \overline{\Delta SL_{i,k}})^2} \sqrt{\sum_{t=1}^T (\Delta SL_{(j,l)}(t) - \overline{\Delta SL_{j,l}})^2}} \quad (1)$$

where t represents the discrete time index (frame number) within a contraction cycle, T is the total number of frames capturing one contraction cycle, and $\overline{\Delta SL}$ denotes the mean value of the sarcomere length change over the cycle.

For each LOI, we calculated two correlation measures. The mutual correlation coefficient r_m measures the synchrony between sarcomeres within the same contraction cycle, calculated as $r_m = \langle r(i, j, k, k) \rangle_{i \neq j}$, where the averaging is performed over all pairs of different sarcomeres ($i \neq j$) within the same contraction cycle k . The serial correlation coefficient r_s quantifies the consistency of individual sarcomeres across different contraction cycles, calculated as $r_s = \langle r(i, i, k, l) \rangle_{k \neq l}$, where the averaging is performed over all pairs of different contraction cycles ($k \neq l$) for the same sarcomere i .

The serial and mutual correlations both were maximal on 5 kPa substrates and declined steadily with increasing substrate stiffness. The decrease of mutual correlation reflects the decrease of synchrony between sarcomeres due to the tug-of-war competition imposed by the rigid constraints on the myofibril level (Fig. 3B). The decrease of serial correlation indicates an increased beat-to-beat variability of the motions of individual sarcomeres (Fig. 3B). Interestingly, the mutual correlation declined more strongly than the serial correlation, by 50% to more than 90% from 5 - 85 kPa.

We introduce the ratio $R = r_m/r_s$ of serial to mutual correlation coefficients to distinguish static from stochastic heterogeneity (Fig. 3B,C). When $R = 1$, the heterogeneity is completely stochastic. Random shuffling of sarcomeres (i, j) and contraction cycles (k, l) would in that case not affect R . When $R \ll 1$, the heterogeneity is largely static. In this case, mutual correlations are much smaller than serial correlations, indicating that the motion varies much more between sarcomeres than for a given sarcomere from one contraction cycle to another (Fig. 3D,E). The broad distribution of R values for all examined LOIs shows that the heterogeneity was neither fully stochastic nor fully static but rather distributed across the full spectrum from stochastic to static (Fig. 3C).

We examined R for different substrate conditions and found a strong dependence on substrate elasticity for both length change and velocity correlations (Fig. 3B). Heterogeneity was mostly stochastic for 5 kPa and 9 kPa substrates and increasingly static for stiffer substrates with non-physiological elasticities.

Sarcomere popping events are stochastically independent and not only occur in structurally “weak” sarcomeres

Beyond the heterogeneous contraction patterns, we observed discrete mechanical instabilities in the form of sudden sarcomere elongations, mostly at the end of contractions, which we termed “popping” events. Defined as sarcomere elongations exceeding $0.25 \mu\text{m}$ (Fig. 3A,F), these events likely represent passive yielding where threshold tension triggers an avalanche-like release of myosin heads while neighboring sarcomeres continue to contract or relax in a more direct manner without overshoot.

The rate of popping events showed a clear dependence on substrate stiffness (Fig. 3G). Stiffer substrates (49-85 kPa) led to higher popping rates than softer substrates (5-15 kPa), with median frequencies increasing from approximately 0.08 events per sarcomere per cycle on soft substrates to over 0.14 on the stiffest substrates. Importantly, even on the softest substrates, popping frequencies remained finite, indicating that sarcomere popping is an intrinsic feature rather than

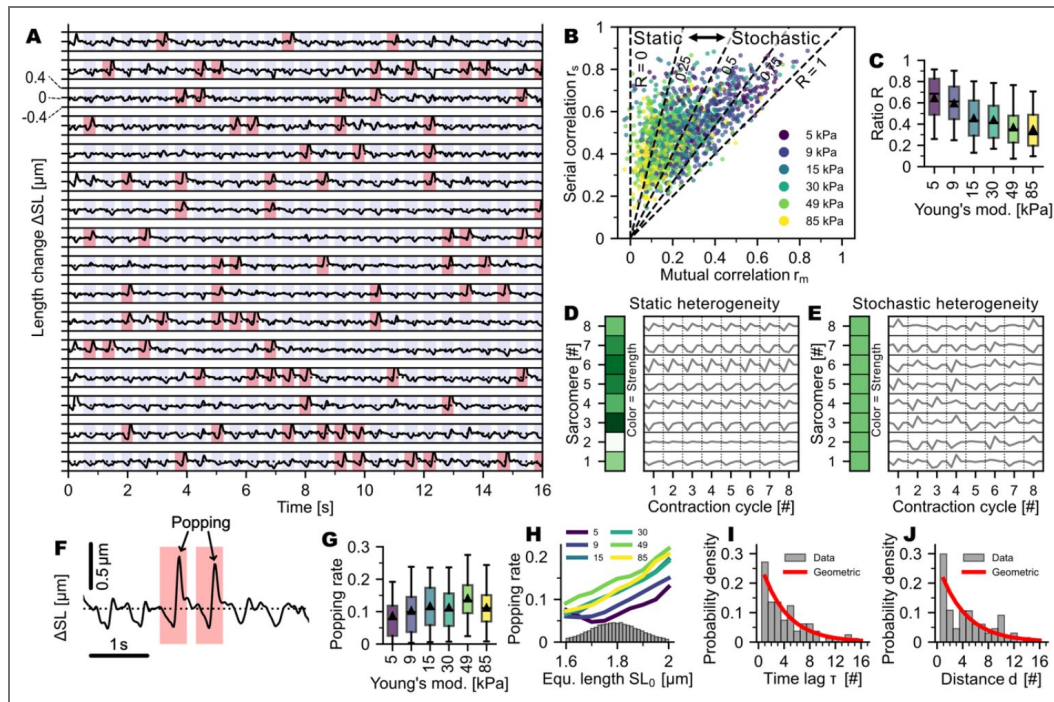


Figure 3. Static versus stochastic heterogeneity in the popping dynamics.

(A) Representative time-series of sarcomere length changes ΔSL of a myofibril in one representative cardiomyocyte on a 30 kPa substrate. Popping events, defined as sarcomere elongations beyond $0.25 \mu\text{m}$ within one contraction cycle, are marked in red. Contraction intervals are marked with a blue background. (B) Correlation analysis showing mutual correlation (r_m) versus serial correlation (r_s). The x-axis shows the mutual correlation of motion between different sarcomeres ($i \neq j$), the y-axis shows the serial correlation of different cycles of one sarcomere ($i = j, k \neq l$). Dashed lines delineate regions of static heterogeneity (left) and stochastic heterogeneity (right). Data points are colored by substrate stiffness (5–85 kPa). (C) Ratio R between average mutual and serial correlation of ΔSL , serving as a measure for the degree of stochasticity in motions, for different substrate stiffnesses. (D,E) Illustrative computer-generated sketches of sarcomere length changes ΔSL in different contraction cycles for purely static heterogeneity (D) and purely stochastic heterogeneity (E). Color bar denotes sarcomere contractile strength. (F) Zoomed view of consecutive experimentally observed contraction cycles showing popping events (red shaded regions) where sarcomeres elongated beyond the threshold of $0.25 \mu\text{m}$ during contraction. (G) Overall popping frequencies for different substrate conditions. (H) Popping frequency as a function of sarcomere equilibrium length SL_0 . Lines show averages for different substrate stiffnesses, with underlying distribution of equilibrium lengths shown below in gray. (I,J) Probability density distributions of time lag (I) and distance (J) between popping events for single LOI compared with corresponding geometric distributions (red lines). **Data and statistics:** Panels B,C,G–J show data from 2,321 LOIs (5 kPa: 184, 9 kPa: 580, 15 kPa: 392, 29 kPa: 319, 49 kPa: 503, 85 kPa: 343). Box plots show quartiles, mean (triangle) and median (line), with whiskers representing the 5th and 95th percentiles. Statistical analysis was performed using Kruskal-Wallis and Dunn's post hoc tests, with significance set at $p < 0.05$. All differences were significant.

a pathological response to specific mechanical conditions. This baseline level of popping across all substrate stiffnesses demonstrates that mechanical instabilities are fundamental to sarcomere dynamics.

Popping frequency also correlated with sarcomere equilibrium length (SL_0), with longer sarcomeres exhibiting higher popping rates across all substrate conditions (Fig. 3H). However, the distribution of equilibrium lengths (gray histogram in Fig. 3H) was relatively tightly centered around 1.8 μm . Crucially, the popping rate remained consistently non-zero also across the entire range of equilibrium lengths, even in LOIs where length variability was minimal. This demonstrates that while resting length heterogeneity contributes to popping behavior, it is not the primary cause of these mechanical instabilities.

To assess the stochastic nature of popping events, we analyzed the distributions of time intervals and spatial distances between consecutive popping events. We assessed the distributions of distance (d) and time gaps (τ) for all LOIs and compared them with geometric distributions $G(k)$ with respective event probabilities (Fig. 3I, J). Using the Kolmogorov-Smirnov test, we could not reject the hypothesis that popping events are stochastically independent for 49% of LOIs with respect to distance and 47% of LOIs with respect to time gaps (p-value = 0.01). This substantial proportion of LOIs showing stochastically independent popping events demonstrates that popping has a stochastic component, independent of deterministic factors such as sarcomere strength heterogeneity or structural variations. While the remaining LOIs show non-random clustering patterns—likely reflecting the influence of local mechanical coupling or morphological heterogeneities—the underlying stochastic mechanism appears to be intrinsic to sarcomere mechanics itself.

A mesoscopic Langevin framework for coupled sarcomere dynamics

To rationalize the observed complex sarcomere dynamics, we developed a model (Fig. 4A) describing the dynamics of each sarcomere i by an underdamped Langevin equation—a second-order stochastic differential equation. We represent a sarcomere mechanically as composed of three parallel components: an active force generator, contributing force $F_{a,i}$, a viscous damper, contributing force $F_{d,i}$, and an elastic element, contributing force $F_{s,i}$. Since we neglect physical mass, forces at all nodes between sarcomeres are instantaneously balanced, meaning every sarcomere experiences the same external load F_m . However, this external load is not instantaneously balanced by the internal forces (F_a, F_d, F_s) within each sarcomere due to the transient nature of the contraction. The resulting force imbalance distributes differently among the three elements from sarcomere to sarcomere, driving asynchronous dynamics (Fig. 4A). To capture this non-equilibrium behavior, we introduce the effective parameter μ , which acts as a quasi-inertial mass. The equation of motion reads:

$$\dot{v}_i = \frac{1}{\mu} [F_a(v_i, c) + F_d(v_i) + F_s(x_i) - F_m(\vec{x})] + \eta(t), \quad \dot{x}_i = v_i \quad (2)$$

where v_i and x_i are velocity and length of sarcomere i , \vec{x} is a vector of all sarcomere lengths, $c(t)$ is the time-dependent activation, and $\eta(t)$ a Gaussian noise term. Multiplying Eq. (2) by μ recovers the form of Newton's second law ($F = m \cdot a$), where $\mu \dot{v}_i$ represents the inertial term. While not a physical mass, μ models the characteristic time scale of the system's kinetic response, reflecting the delayed attachment and detachment rates of actomyosin cross-bridges. This parameter defines how fast the system is drawn to the nullcline determined by the force balance, effectively smoothing instantaneous force fluctuations, representing the system's persistence against rapid force changes.

This phenomenological underdamped Langevin framework, previously successfully applied to nonlinear systems in general¹⁹ and to cell migration in particular^{20,21}, captures the nonlinear dynamics and emergent collective behaviors observed in our sarcomere system without explicitly

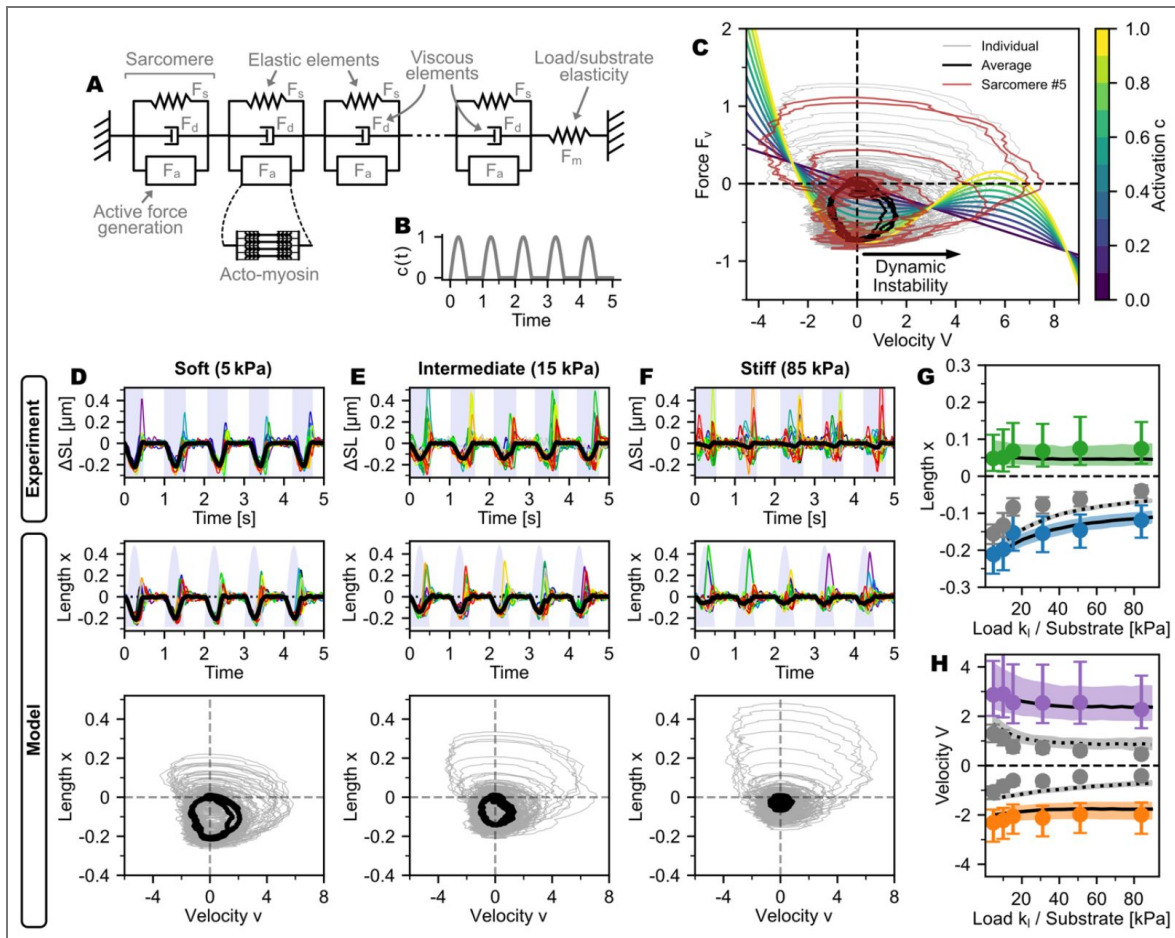


Figure 4. Mesoscopic model of coupled sarcomeres with non-monotonic force-velocity dynamics and comparison with data.

(A) Schematic of the myofibril model where each sarcomere comprises three parallel components: an active force generator, creating force F_a , a viscous element creating force F_d , and passive elastic element, creating force F_s . Sarcomeres are mechanically coupled in series; such that an external force F_m generated by elastic substrate deformation is transmitted uniformly through all sarcomeres in the chain. (B) Activation imposes a time-dependent modulation of the active force throughout the contraction cycles, with a waveform $c(t)$. (C) Smooth curves: Activation-dependent force-velocity curves showing an S-shaped non-monotonic relationship with two stable branches and an unstable region with a negative-slope; the force-velocity relations are color-coded by activation level. Superimposed trajectories (gray) are trajectories of 20 individual sarcomeres, generated by Eq. 2. The black trajectory is the myofibril average, and one sarcomere is highlighted in red. (D-F) Experimental recordings and corresponding model outputs for cells on soft (5 kPa), intermediate (15 kPa), and stiff (85 kPa) substrates showing timeseries of ΔSL /length x with blue-shaded contraction intervals (experiment) or $c(t)$ (model), together with the associated v - x trajectories in phase space; colored traces depict individual sarcomeres, and black traces denote cycle averages. (G-H) Extrema (maximum and minimum) of length x and velocity v per contraction cycle for individual sarcomeres and for the myofibril average as a function of substrate stiffness k_i ; dashed lines indicate the average, solid lines show individual-sarcomere values, colored shaded regions denote the standard deviation, and points with error bars display the experimental data median and inter-quantile range.

modeling the underlying molecular mechanisms. This makes it particularly well-suited for studying the emergence of complex, large-scale behavior from fundamental single-sarcomere interactions.

To model the active actomyosin force F_a , we chose the 3rd order polynomial ansatz, while the viscous drag F_d is modeled as a linear friction term:

$$F_a(v_i, x_i, c) = (f_0 + f_1 v + f_2 v^2 + f_3 v^3) \cdot c(t) \quad (3)$$

$$F_d(v_i) = -\gamma_s v_i \quad (4)$$

The polynomial in Eq. (3) is a generalist functional form capable of capturing a broad spectrum of force-velocity relationships. Multiplying by the time-dependent activation $c(t)$ makes sure that active force generation scales with calcium availability, reflecting troponin C binding and the resulting availability of myosin binding sites on actin². At high activation ($c \approx 1$), F_a drives contraction, while at low activation ($c \approx 0$), the viscous drag F_d dominates, governing passive relaxation dynamics.

In our model, as in previous work²², we represent the passive elastic element inside each sarcomere i using a piecewise defined function, allowing for different behaviors for shortening and lengthening. We here assume that elastic resistance during shortening is linear (provided by, e.g., microtubules²³) and quadratic during lengthening (provided by, e.g., titin²²):

$$F_{s,i}(x_i) = \begin{cases} -k_1 \cdot x_i & \text{for } x_i < 0 \text{ (shortening)} \\ -k_1 \cdot x_i - k_2 \cdot x_i^2 & \text{for } x_i \geq 0 \text{ (lengthening)} \end{cases} \quad (5)$$

Here, k_1 and k_2 are elastic constants. For simplicity and without loss of generality, we set the sarcomere equilibrium length to zero ($x_{eq} = 0$). For serially coupled sarcomeres, the total elastic force on each sarcomere is $F_{p,i}(\vec{x}) = F_{s,i}(x_i) - F_m(\vec{x})$ where $F_m(\vec{x})$ is the external myofibril load. For our experiment of single hiPSC-derived cardiomyocytes on micropatterned elastic soft gels, we assume an auxotonic load $F_m(\vec{x}) = -k_l \cdot x_m$ with myofibril length change $x_m = \sum_j x_j$ and elasticity k_l .

We model stochastic fluctuations on the sarcomere level through the random noise term $\eta(t) = \eta_t(t) + \eta_a(t)$. This term combines two distinct components: thermal noise $\eta_t(t)$ and active noise $\eta_a(t)$, originating from the stochastic dynamics of the collective action of the myosin motors in the sarcomere. As shown previously²⁴, these fluctuations arising from the stochastic motor kinetics can be approximated as delta-correlated:

$$\langle \eta_a(t) \eta_a(0) \rangle \simeq \eta_{a,0} n r (1 - r) \delta(t) \quad (6)$$

with system-specific magnitude $\eta_{a,0}$, the fraction of active motors n and the duty ratio of motors r . These fluctuations originate from the discrete, stochastic switching of individual motors between bound and unbound states²⁴. For the active fluctuations, we model n with a sigmoidal function with steepness β dependent on velocity v dependent on activation $c(t)$, assuming active shortening and passive elongation of sarcomeres:

$$n(v, c) = \frac{1}{1 + \exp(-v\beta)} \cdot c(t) \quad (7)$$

Data-driven parameter optimization reproduces complex sarcomere dynamics

Our model comprises 10 parameters. To specify the parameters, we simulated 20 serially connected sarcomeres over 10 contraction cycles using the Euler-Maruyama scheme²⁵. The cyclic activation was modeled using a simplified custom activation function $c(t)$ based on a clipped sine with a beating rate matching the experimental data (Fig. 4B). Since analytical fitting of such non-linear, stochastic and time-dependent systems to experimental data is impossible, we employed Differential Evolution²⁶, a robust gradient-free optimization method, to identify the physical parameters generating the experimentally observed dynamics. The objective was to minimize a loss function based on the Kolmogorov-Smirnov (KS) coefficient, which quantifies the similarity between the distributions of simulated and experimental data on a scale from 0 (identical) to 1 (no overlap).

The model evaluation compared the distributions of sarcomere length changes and velocities from simulations with representative experimental LOIs from substrates (5, 15, and 85 kPa) covering the full range of mechanical loads. To account for the transient activation dependency, we divided the trajectories into four distinct phases: quiescent, early activation, mid-activation, and late activation, and compared the distributions for each phase using the KS metric. To match the experimental temporal resolution, model data was subsampled to 16 ms frame intervals. For each parameter set during optimization, all three substrate conditions were simulated, and the KS coefficient was computed for each condition and phase. The final loss was then calculated as the mean loss over all three conditions and four contraction phases, yielding a single metric quantifying the overall model-experiment agreement. The 10 model parameters were optimized within prespecified bounds (Table S2).

This optimization process yielded a model in excellent agreement with the experimental data (Fig. 4D-F). The average KS coefficient across all conditions and phases was ~ 0.05 , confirming a high degree of similarity between the simulated and measured distributions of individual sarcomere lengths. Ultimately, we inferred a single, unified model capable of replicating dynamics across all substrate elasticities by adjusting only the substrate stiffness parameter. The model correctly captures the extremal trends (minima and maxima) of decreasing sarcomere displacement and velocity with increasing substrate stiffness at both the individual and average sarcomere levels (Fig. 4G, H). While the model predicts slightly stronger average contraction and velocity extrema than measured, the stiffness dependence of these extrema is consistent with experimental observations (gray data in Fig. 4G, H). Note that the model correctly replicates the emergence of smooth and periodic contraction at the myofibril level from the highly stochastic and heterogeneous dynamics of individual sarcomeres (Fig. 4D-F).

Non-monotonic force-velocity dynamics drive tug-of-war and limit cycles in coupled sarcomeres

Our data-driven inference procedure reveals, without making this an *a priori* assumption, that the active force F_a exhibits a non-monotonic force-velocity relationship (Fig. 4C, Movie S2), with branches separated by an unstable region of negative slope ($dF/dv < 0$), corresponding to negative friction. This relationship is dynamically modulated by the activation $c(t)$, creating a complex time-dependent force landscape that governs sarcomere behavior.

The model is effectively analogous to a Van-der-Pol relaxation oscillator in force-velocity space¹⁹. As total myofibril shortening proceeds, the external mechanical load from the substrate increases, slowing down contraction velocities of all sarcomeres. The non-monotonic force-velocity relationship implies that there is an intrinsic threshold force at which sarcomeres become dynamically unstable. Physically, this corresponds to a tipping point where the stochastic unbinding of a few myosin cross-bridges triggers an avalanche-like release of the remaining more strongly loaded cross-bridges, switching the sarcomere from contraction to rapid elongation.

This instability has different consequences in the different phases of the contraction cycle: During the initial contraction phase, joint sarcomere shortening drives the velocity toward the instability threshold. Through dynamic selection, stochastic fluctuations (modeled by η) then push random

sarcomeres past the tipping point. Because activation remains high, this elongation is transient; as a particular sarcomere lengthens, load quickly redistributes to its passive elements and while other sarcomeres take up the slack, it ends up back on the contracting branch. This rapid switching generates the stable limit-cycle oscillations observed in individual sarcomeres (Fig. 2H-J).

During relaxation (declining activation), the instability threshold decreases (Fig. 4C). On stiff substrates, where external load remains high, this lower threshold causes a larger fraction of sarcomeres to slip past the instability point. Unlike in the first regime, the declining active force allows for large, sustained “popping” excursions (Fig. 4D-F). We observed that only a subset of sarcomeres pop (~10%), which effectively buffers the load for the remaining sarcomeres, allowing them to relax smoothly without over-extension.

Stochastic fluctuations $\eta(t)$ (Eq. 6) are essential to reproduce the heterogeneous sarcomere behavior seen experimentally, including beat-to-beat variability, competition, and popping events. Removing the stochastic drive from the equation of motion (Eq. 2) in simulations collapses trajectories, inconsistent with experiments (Fig. 5A,B). To probe robustness against fixed force non-uniformities, we introduced static variability by scaled each sarcomere's active force F_a with a constant, factor drawn for each sarcomere in the chain of 20 from a distribution with standard deviation σ_a . Functionally, this assigns each sarcomere a slightly different maximum force threshold. This force variability alone biases trajectories and creates deterministic static heterogeneity during contraction according to each sarcomere's strength (Fig. 5C), also inconsistent with our data. Adding stochastic fluctuations leads to trajectories most closely resembling the experimental data (Fig. 5D).

Correlation analysis (Fig. 5E; compare with experimental data in Fig. 3B) of the simulated data with different levels of static heterogeneity σ_a shows, as expected, that without stochastic fluctuations, the serial correlation of sarcomeres is always 1, meaning that individual sarcomeres always behave the same way through contraction cycles. In contrast, simulations with stochastic fluctuations maintain stochastic heterogeneity ($R > 0.8$) even with substantial static force heterogeneity (up to $\sigma_a \approx 0.2$) (Fig. 5E).

Discussion

We combined high-speed imaging of human induced pluripotent stem cell (iPSC)-derived cardiomyocytes with detailed AI-based quantitative analysis. We discovered rich subcellular dynamics that remain hidden at the whole-cell level. While overall cell contraction cycles were regular, individual sarcomeres displayed rapid oscillations, reversible popping events, and stochastic beat-to-beat variability within the same myofibril. Increased substrate stiffness reduced overall cell contraction amplitudes, but had only a weak effect on single-sarcomere length-changes and contraction velocities. Rigid substrates instead promoted tug-of-war-like interactions and loss of synchrony between sarcomeres along myofibrils.

To interpret these observations mechanistically, we developed a data-driven, mesoscopic modeling framework describing transient, non-equilibrium dynamics and mechanical coupling among serially connected sarcomeres. The model relies on two components that accurately reproduce the experimentally observed dynamics: a non-monotonic force-velocity relationship that generates a dynamic instability at a critical force and intrinsic stochastic force fluctuations at the sarcomere level. This approach differs from classical modeling of skeletal muscle based on a force-length relationship. We find that our model is more appropriate than such models for cardiomyocytes that operate in a regime of rapid transient activation-relaxation cycles, viscous drag, and velocity-dependent force generation.

The dynamic instability central to our framework arises from the non-monotonic shape of the force-velocity relationship. Note that this functional form was not an initial assumption but that it emerged when optimizing the parameters of the very general modeling ansatz to fit our experimental data. This result connects to foundational, reductionist theories of coupled molecular motors working against an external load²⁷⁻³⁰, which predict that at a critical load, a

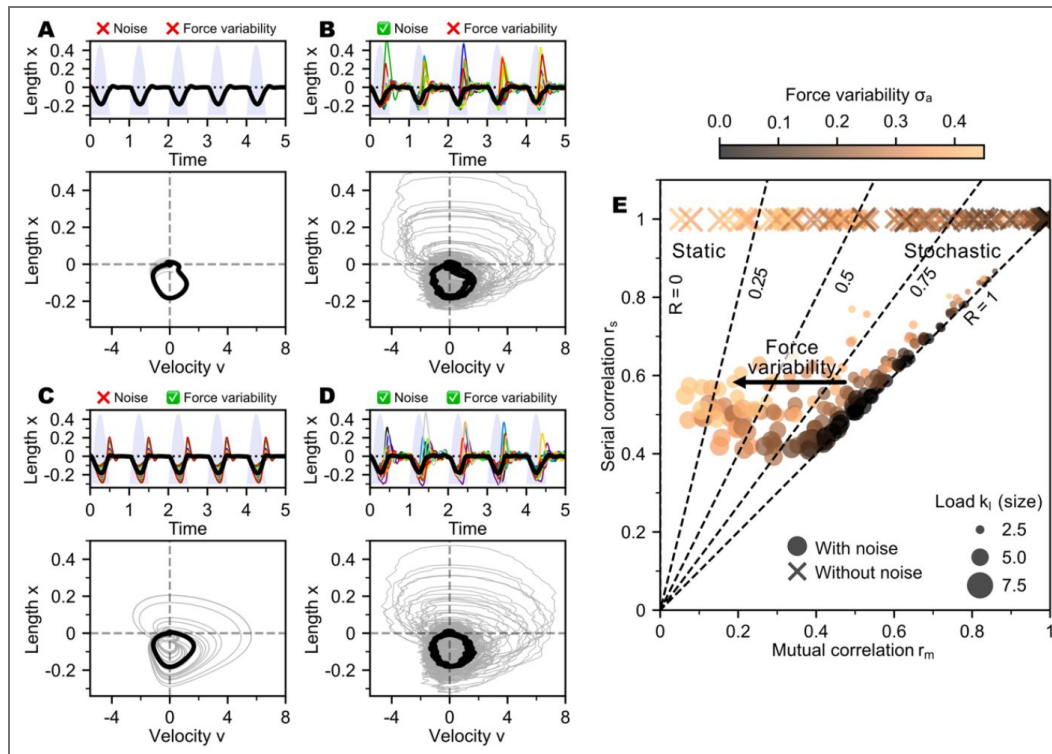


Figure 5. Simulation of static and stochastic heterogeneity in sarcomere dynamics.

(A-D) Top panels: overlaid timeseries of individual sarcomere length changes (colored curves) and the ensemble average (thick black curve). Bottom panels: trajectories in phase space (length change vs. velocity) of individual sarcomeres (gray) and ensemble average (black). (A) Uniform ensemble (no noise, no force variability). (B) Stochastic heterogeneity driven by noise only. (C) Static heterogeneity driven by intrinsic force variability (σ_a) only. (D) Mixed, static and stochastic heterogeneity with both noise and force variability. (E) Serial correlation r_s versus mutual correlation r_m across load levels and force variability; marker size encodes the dimensionless simulated substrate stiffness k_l , and color shade indicates the standard deviation of the multiplicative factor modulating each sarcomere's active force. Dashed lines mark the transition from purely static heterogeneity ($R = 0$) to purely stochastic heterogeneity ($R = 1$). Circles denote simulations with noise/stochastic fluctuations, and crosses denote deterministic simulations without noise/stochastic fluctuations.

collective, avalanche-like unbinding of motors from their track (e.g. myosin heads from actin in a sarcomere) induces a dynamic phase transition from active forward motion against the load to rapid passive slipping. Such instabilities have so far only been reported in reconstituted motility assays^{29,31}. We have here observed an analogous instability in cardiomyocytes manifesting itself in the observed switching between contraction and expansion and the popping events of individual sarcomeres. If sarcomeres followed a monotonic force-velocity relationship, increasing load would simply cause uniform slowing or stalling. Small non-uniformities caused by fluctuations would decay, returning the system to a uniform state. The non-monotonic force-velocity relationship, instead, amplifies such fluctuations, driving the system into limit cycles that produce the high-frequency oscillations and stochastic heterogeneity we observe (Fig. 2G [↗](#)).

What could be the physiological roles of the observed phenomena? The popping events are the most dramatic outcome of the instability-amplified stochastic noise. Their reversible nature, ubiquity across all tested conditions, and prevalence at the end of contractions - where declining activation reduces the fraction of attached cross-bridges - are all consistent with a dynamic instability rather than structural failure. We therefore view popping as an intrinsic outcome of transient, non-equilibrium sarcomere dynamics. While possibly similar popping has been described in skeletal muscle³², particularly in the context of residual force enhancement³³, the observation in rhythmically contracting cardiomyocytes is a key new finding of this study. A physiological function of popping might be that intermittent yielding in a subset of sarcomeres accelerates myofibril-level relaxation toward the onset of the next diastole, helping tension decay even while individual sarcomere lengths remain non-uniform. A physiological role of stochastic heterogeneity of yielding might be the limitation of sarcomere damage. Our data indicate a mixture of static and stochastic heterogeneity. Some sarcomeres exhibit persistent differences suggestive of structural or compositional non-uniformities, yet many myofibrils show strong, cycle-to-cycle stochastic variability, including popping. As our simulations demonstrate, even in the presence of low to moderate sarcomere strength variability, the interplay between stochastic fluctuations and the dynamic instability prevents deterministic yielding. The interplay between intrinsic fluctuations and the dynamic instability randomizes yielding events across cycles and sarcomeres, preventing the repetitive overload of any single element and reducing the likelihood of localized damage.

Stochastic heterogeneity thus provides a robust mechanism for maintaining structural and functional homeostasis. Healthy adult cardiomyocytes—with their more ordered myofibril and sarcomere architecture compared with stem-cell-derived cardiomyocytes³⁴—are expected to show smaller static non-uniformities while still exhibiting stochastic heterogeneity. While speculative for human cardiomyocytes, this hypothesis is supported by in-situ measurements of single-sarcomere dynamics in mouse myocardium, which found stochastic heterogeneity⁶.

In diseased and disordered myofibrils, static non-uniformities may overwhelm the protective stochastic mechanism^{14,34,35} and instability may then be consistently triggered at the most vulnerable sarcomeres, concentrating mechanical stress and leading to fatigue and maladaptive remodeling. This perspective provides a more nuanced view than those based on fixed “weak-strong” contrasts¹⁴, suggesting that pathology may arise from local structural weakness, but that that weakness would have to overwhelm the protective load-sharing mechanism. The phenomenon that amplified random noise can enhance responsiveness and stabilize dynamics has also been described in systems showing stochastic resonance³⁶.

The presented framework is mesoscopic by design, omitting explicit molecular details such as calcium kinetics or individual cross-bridge states. Instead, we adopted a top-down approach, inferring the emergent mesoscopic physics directly from the experimental data. We utilized a mesoscopic Langevin framework in the hydrodynamic limit, where the deterministic force term represents the collective average of the underlying molecular kinetics and mechanical interactions, while the stochastic term accounts for unresolved microscopic fluctuations, following the general principles of active matter theory applied to actomyosin systems^{37,38}. The strength of this coarse-grained approach is that it reveals emergent physical principles—such as the non-

monotonic force-velocity relationship—that would remain obscured in parameter-heavy molecular models. The model's predictive power, with only 10 parameters capturing dynamics across three substrate stiffnesses and four contraction phases, validates this strategy.

Our combined experimental and modeling platform offers a powerful tool to dissect the specific molecular drivers of collective sarcomere dynamics in future studies. By applying pharmacological perturbations or specific mutations, one could link distinct molecular defects — such as altered cross-bridge kinetics, calcium sensitivity, or titin stiffness — to quantitative changes in the model's physical parameters. This would establish a rigorous mapping between molecular function and myofibril stability, enabling a systematic analysis of how specific pathologies disrupt the contractile homeostasis of the heart.

Materials and Methods

Generation and culturing of hiPSC ACTN2-Citrine-derived cardiomyocytes

Cardiomyocyte differentiation of a ACTN2-Citrine reporter hiPSC line³⁹ was performed according to Tiburcy *et al.*⁴⁰. hiPSC-ACTN2-Citrine-derived cardiomyocytes were cultured in 6 well plates (Cat 3516, Corning) in serum-free “cardio” medium (0.4 mM Ca²⁺, RPMI 1640 with GlutaMAX (Cat 61870, Invitrogen), 1% Penicillin/Streptomycin (Cat 15140, Invitrogen), 2% B27 supplement (Cat 17504-044, Invitrogen) at 37 °C in a 5% CO₂ incubator with culture medium changes at every other day. For re-seeding, cells were detached using Accutase[®] digestion medium (StemPro[®] Accutase[®] cell dissociation reagent (Cat A11105-01, Gibco), 0.025% Trypsin (Cat 15090-046, Gibco), 20 µg/mL DNaseI (Cat 260913, Calbiochem) for 15-20 min at 37°C. Digestion was stopped using “cardio” medium supplemented with 5 µmol/L Rock Inhibitor (Stemolecule Y27632, Cat 04-0012-10, Reprocell) three times the volume of the Accutase[®] mix. Cell clumps were separated using a 100 µm cell strainer. Cells were seeded using ~150,000 cells per micropatterned substrate of ~1 cm² size and cultured 24 hours in “cardio” medium with 5 µmol/L Rock Inhibitor. Cardiomyocytes on soft gels were maintained in serum-free “cardio” medium with daily medium changes at 37 °C in a 5% CO₂ incubator for up to 30 days. Cardiomyocytes were imaged after a maturation period of 20-30 days post seeding on the soft gels.

Sample preparation and measurement

For live-cell video imaging, the soft substrates were mounted in a custom-built holder for round Ø25 mm glass cover slides with serum-free medium. Movies of beating cardiomyocytes were obtained with a confocal microscope (TCS SP5 II, Leica, Germany) at 37°C and 5% CO₂. We used an 8,000 Hz resonant scanner with bidirectional scanning mode and recorded up to 20-30 s long movies of 1024 × 200 pixels at 67 frames per second, i.e. a temporal resolution of 15 ms.

Fabrication of cell-adhesive micropatterns on polyacrylamide soft gels

Silicon wafers (Microchemicals GmbH, Ulm, Germany) were coated with SU-8 photoresist (Series 3005, MicroChem, Newton, USA) using a two-step spin-coating process. The wafers were then exposed to UV light through custom photomasks (Compugraphics, Jena, Germany) and developed to create photoresist masters (details in Ref.³⁹). Polydimethylsiloxane (PDMS) stamps were produced by mixing PDMS and curing agent 10:1 (Sylgard 184 kit, Dow Corning) and pouring it onto the photoresist masters. After degassing and curing, the PDMS was cut and peeled off to create the stamps. Micropatterned polyacrylamide gels were prepared by treating PDMS stamps with plasma to make them hydrophilic, then incubating them with 0.1 mg/ml Synthmax™ (Cat 3535, Corning). The protein-coated stamps were placed on plasma-cleaned glass coverslips and weighted to transfer the protein. Gel solutions of acrylamide and bis-acrylamide were prepared to

achieve different elastic moduli (Table S1 [↗](#)), measured with a rheometer (Physica MCR 501 Rheometer, Anton Paar, Austria). The gel solution was polymerized with the Synthemax-patterned glass on top. The gels were stored in PBS, then washed before use.

Microscopy data analysis and statistical analysis

For processing of the live-cell confocal movies, and tracking and analysis of sarcomere trajectories, our Python package SarcAsM (Sarcomere Analysis Multitool) was used¹⁵. All additional analyses and illustrations were created using custom scripts written in Python. All data is displayed as mean \pm standard deviation unless indicated otherwise. Whenever applicable, we employed the Kruskal-Wallis test, a non-parametric method, for hypothesis testing, and proceeded to a post-hoc multi-comparison using Dunn's test, setting the threshold for statistical significance at a p-value of less than 0.01. All condition differences were deemed significant except where explicitly marked as not significant (n.s.).

Computational model

We implemented the mesoscopic model of coupled sarcomeres in Python 3.12, making use of the NumPy⁴¹ and SciPy⁴² libraries. The model describes sarcomere dynamics through serially coupled underdamped Langevin equations, which is an approach suited to capturing emergent collective behaviors at the myofibril scale without explicitly modelling molecular-level details. We solved the system of stochastic differential equations numerically using the Euler-Maruyama scheme²⁵ with a time step of 2 ms. The dimensionless load parameter k_m was provided as a simulation input, defined for simplicity as 0.1 times the substrate elasticity (in kPa). The remaining model parameters were estimated using Differential Evolution²⁶, a global optimization algorithm, to minimize the Kolmogorov-Smirnov distance between simulated and experimental distributions.

Data availability

All data, analysis scripts, and source code supporting this study are publicly available. The primary software packages developed for this research, SarcAsM and the computational model, are available on GitHub at <https://github.com/danihae/SarcAsM> [↗](#) and <https://github.com/danihae/SarcomereModel> [↗](#), respectively. The complete experimental dataset, alongside code to reproduce the analyses in this manuscript, is archived on Zenodo (<https://doi.org/10.5281/zenodo.17564384> [↗](#)). This repository includes a representative dataset of 25 raw microscopy movies with their corresponding processed line-of-interest (LOI) sarcomere trajectories for each of the six substrate stiffness conditions, as well as the aggregated data frame used to generate all figures.

Acknowledgements

We thank Florian Rehfeldt, Andrei Vilfan, Lev Truskinowsky, David Brückner, Chase Broedersz and Pierre Ronceray for helpful discussions. We gratefully acknowledge the use of the microscopy facility of the Max Planck Institute for Multidisciplinary Sciences for access to cell culture and high-speed confocal microscopy. CFS and DH would like to thank the Isaac Newton Institute for Mathematical Sciences for support and hospitality during the program “New statistical physics in living matter: non equilibrium states under adaptive control”. DH acknowledges the support from the German Academic Foundation (Studienstiftung des Deutschen Volkes) for providing a doctoral fellowship and the Campus Institute for Data Science (CIDAS) at the University of Göttingen for awarding a postdoctoral fellowship. The research of CFS was supported by the European Research Council under the European Union's Seventh Framework Program (FP7/2007-2013) with the ERC grant agreement n°340528. WHZ acknowledges the support from the DZHK (German Center for Cardiovascular Research), the German Federal Ministry of Education and Research (IndiHEART; 161L0250A), the German Research Foundation (DFG SFB 1002 C04/S01, IRTG 1816, RTG 2824, EXC 2067-1), and the Fondation Leducq (20CVD04).

Additional information

Author contributions


D.H., T.D., W.H.Z. and C.F.S. conceived and designed the study. D.H., L.H., and T.D. developed the methodology. W.H.Z. and C.F.S. supplied the essential resources. D.H., L.H., and T.D. performed micropatterning and cardiomyocyte experiments. D.H. and K.N. analyzed experimental data. D.H. conceived and implemented the theoretical model. D.H. created the visualizations. The original draft was written by D.H., and all authors contributed to the review and editing of the manuscript.

Funding

| Funder | Grant reference number | Author |
|---|------------------------|---------------------|
| EC European Research Council (ERC) | 340528 | Christoph F Schmidt |
| German Center for Cardiovascular Research | | Wolfram Zimmermann |
| German Academic Foundation | | Daniel Haertter |
| Campus Institute for Data Science | | Daniel Haertter |
| German Federal Ministry of Education and Research | IndiHEART; 161L0250A | Wolfram Zimmermann |
| German Research Foundation | DFG SFB 1002 C04/S01 | Wolfram Zimmermann |
| German Research Foundation | IRTG 1816 | Wolfram Zimmermann |
| German Research Foundation | RTG 2824 | Wolfram Zimmermann |
| German Research Foundation | EXC 2067-1 | Wolfram Zimmermann |
| Fondation Leducq (Leducq Foundation) | 20CVD04 | Wolfram Zimmermann |

Author ORCID iDs

Daniel Haertter:  <https://orcid.org/0000-0002-9582-6141>

Kengo Nishi:  <https://orcid.org/0000-0003-3488-402X>

Christoph F Schmidt:  <https://orcid.org/0000-0003-2864-6973>

Additional files

[Supplemental Information](#) 

[Movie1](#) 

[Movie2](#) 

References

1. Maack C., et al. (2019) Treatments targeting inotropy. *Eur. Heart J* **40**:3626-3644 <https://doi.org/10.1093/eurheartj/ehy600> | [PubMed](#)
2. Spudich J. A. (2001) The myosin swinging cross-bridge model. *Nat. Rev. Mol. Cell Biol* **2**:387-392 <https://doi.org/10.1038/35073086> | [PubMed](#)
3. Huxley A. F., Simmons R. M. (1971) Proposed Mechanism of Force Generation in Striated Muscle. *Nature* **233**:533-538 <https://doi.org/10.1038/233533a0> | [PubMed](#)

4. **Gordon A. M.**, Huxley A. F., Julian F. J. (1966) The variation in isometric tension with sarcomere length in vertebrate muscle fibres. *J. Physiol* **184**:170-192 <https://doi.org/10.1113/jphysiol.1966.sp007909> | [PubMed](#)
5. **Rassier D. E.** (2017) Sarcomere mechanics in striated muscles: from molecules to sarcomeres to cells. *Am. J. Physiol.-Cell Physiol* **313**:C134-C145 <https://doi.org/10.1152/ajpcell.00050.2017> | [PubMed](#)
6. **Kobirumaki-Shimozawa F.**, et al. (2021) Synchrony of sarcomeric movement regulates left ventricular pump function in the in vivo beating mouse heart. *J. Gen. Physiol* **153**:e202012860 <https://doi.org/10.1085/jgp.202012860> | [PubMed](#)
7. **Li J.**, et al. (2023) Stretch Harmonizes Sarcomere Strain Across the Cardiomyocyte. *Circ. Res* **133**:255-270 <https://doi.org/10.1161/circresaha.123.322588> | [PubMed](#)
8. **Kobirumaki-Shimozawa F.**, Oyama K., Nakanishi T., Ishiwata S., Fukuda N. (2024) Asynchronous movement of sarcomeres in myocardium under living conditions: role of titin. *Front. Physiol* **15** <https://doi.org/10.3389/fphys.2024.1426545> | [PubMed](#)
9. **Edman K. A. P.** (1980) The role of non-uniform sarcomere behaviour during relaxation of striated muscle. *Eur. Heart J* **1**:49-57 https://doi.org/10.1093/eurheartj/1.suppl_1.49 | [PubMed](#)
10. **Telley I. A.**, Denoth J., Ranatunga K. W. (2003) Inter-Sarcomere Dynamics in Muscle Fibres. In: Sugi H. (Ed). *Molecular and Cellular Aspects of Muscle Contraction* **538** Boston, MA: Springer US. pp. 481-500 https://doi.org/10.1007/978-1-4419-9029-7_44 | [PubMed](#)
11. **Moo E. K.**, Leonard T. R., Herzog W. (2017) In Vivo Sarcomere Lengths Become More Non-uniform upon Activation in Intact Whole Muscle. *Front. Physiol* **8**:1015 <https://doi.org/10.3389/fphys.2017.01015> | [PubMed](#)
12. **Givli S.** (2010) Towards multi-scale modeling of muscle fibers with sarcomere non-uniformities. *J. Theor. Biol* **264**:882-892 <https://doi.org/10.1016/j.jtbi.2010.02.048> | [PubMed](#)
13. **de Tombe P. P.**, et al. (2010) Myofilament length dependent activation. *J. Mol. Cell. Cardiol* **48**:851-858 <https://doi.org/10.1016/j.yjmcc.2009.12.017> | [PubMed](#)
14. **Månsson A.** (2014) Hypothesis and theory: mechanical instabilities and non-uniformities in hereditary sarcomere myopathies. *Front. Physiol* **5** <https://doi.org/10.3389/fphys.2014.00350> | [PubMed](#)
15. **Haertter D.**, et al. (2025) SarcAsM: AI-based multiscale analysis of sarcomere organization and contractility in cardiomyocytes. *bioRxiv* <https://doi.org/10.1101/2025.04.29.650605>
16. **Ribeiro A. J. S.**, et al. (2015) Contractility of single cardiomyocytes differentiated from pluripotent stem cells depends on physiological shape and substrate stiffness. *Proc. Natl. Acad. Sci* **112**:12705-12710 <https://doi.org/10.1073/pnas.1508073112> | [PubMed](#)
17. **Engler A. J.**, et al. (2008) Embryonic cardiomyocytes beat best on a matrix with heart-like elasticity: scar-like rigidity inhibits beating. *J. Cell Sci* **121**:3794-3802 <https://doi.org/10.1242/jcs.029678> | [PubMed](#)
18. **Hazeltine L. B.**, et al. (2012) Effects of Substrate Mechanics on Contractility of Cardiomyocytes Generated from Human Pluripotent Stem Cells. *Int. J. Cell Biol* **2012**:1-13 <https://doi.org/10.1155/2012/508294> | [PubMed](#)
19. **Strogatz S. H.** (2018) *Nonlinear Dynamics and Chaos: With Applications to Physics, Biology, Chemistry, and Engineering* CRC Press.
20. **Brückner D. B.**, et al. (2019) Stochastic nonlinear dynamics of confined cell migration in two-state systems. *Nat. Phys* **15**:595-601 <https://doi.org/10.1038/s41567-019-0445-4>
21. **Brückner D. B.**, et al. (2021) Learning the dynamics of cell-cell interactions in confined cell migration. *Proc. Natl. Acad. Sci* **118**:e2016602118 <https://doi.org/10.1073/pnas.2016602118> | [PubMed](#)
22. **Loescher C. M.**, et al. (2023) Titin governs myocardial passive stiffness with major support from microtubules and actin and the extracellular matrix. *Nat. Cardiovasc. Res* 1-12 <https://doi.org/10.1038/s44161-023-00348-1> | [PubMed](#)

23. Prosser B. L. (2023) Pinpointing the contributors to myocardial passive stiffness. *Nat. Cardiovasc. Res* **2**:962-963 <https://doi.org/10.1038/s44161-023-00350-7> | PubMed
24. Nadrowski B., Martin P., Jülicher F. (2004) Active hair-bundle motility harnesses noise to operate near an optimum of mechanosensitivity. *Proc. Natl. Acad. Sci* **101**:12195-12200 <https://doi.org/10.1073/pnas.0403020101> | PubMed
25. Kloeden P. E., Platen E. (1992) Introduction to Stochastic Time Discrete Approximation. In: Kloeden P. E., Platen E. (Eds). *Numerical Solution of Stochastic Differential Equations* Berlin, Heidelberg: Springer. pp. 305-337 https://doi.org/10.1007/978-3-662-12616-5_9
26. Storn R., Price K. (1997) Differential Evolution - A Simple and Efficient Heuristic for global Optimization over Continuous Spaces. *J. Glob. Optim* **11**:341-359 <https://doi.org/10.1023/a:1008202821328>
27. Jülicher F., Prost J. (1997) Spontaneous Oscillations of Collective Molecular Motors. *Phys. Rev. Lett* **78**:4510-4513 <https://doi.org/10.1103/physrevlett.78.4510>
28. Guérin T., Prost J., Martin P., Joanny J.-F. (2010) Coordination and collective properties of molecular motors: theory. *Curr. Opin. Cell Biol* **22**:14-20 <https://doi.org/10.1016/j.ceb.2009.12.012> | PubMed
29. Plaçais P.-Y., Balland M., Guérin T., Joanny J.-F., Martin P. (2009) Spontaneous Oscillations of a Minimal Actomyosin System under Elastic Loading. *Phys. Rev. Lett* **103**:158102 <https://doi.org/10.1103/physrevlett.103.158102> | PubMed
30. Walcott S., Sun S. X. (2009) Hysteresis in cross-bridge models of muscle. *Phys. Chem. Chem. Phys* **11**:4871 <https://doi.org/10.1039/b900551j> | PubMed
31. Riveline D., et al. (1998) Acting on actin: the electric motility assay. *Eur. Biophys. J* **27**:403-408 <https://doi.org/10.1007/s002490050147> | PubMed
32. Morgan D. L., Proske U. (2006) Sarcomere popping requires stretch over a range where total tension decreases with length. *J. Physiol* **574**:627-628 <https://doi.org/10.1113/jphysiol.2006.574201> | PubMed
33. Johnston K., Jinha A., Herzog W. (2016) The role of sarcomere length non-uniformities in residual force enhancement of skeletal muscle myofibrils. *R Soc Open Sci* **3**:150657 <https://doi.org/10.1098/rsos.150657> | PubMed
34. Wadmore K., Azad A. J., Gehmlich K. (2021) The Role of Z-disc Proteins in Myopathy and Cardiomyopathy. *Int. J. Mol. Sci* **22**:3058 <https://doi.org/10.3390/ijms22063058> | PubMed
35. Fomin A., et al. (2021) Truncated titin proteins and titin haploinsufficiency are targets for functional recovery in human cardiomyopathy due to TTN mutations. *Sci. Transl. Med* **13**:eabd3079 <https://doi.org/10.1126/scitranslmed.abd3079> | PubMed
36. McDonnell M. D., Abbott D. (2009) What Is Stochastic Resonance? Definitions, Misconceptions, Debates, and Its Relevance to Biology. *PLOS Comput. Biol* **5**:e1000348 <https://doi.org/10.1371/journal.pcbi.1000348> | PubMed
37. Jülicher F., Kruse K., Prost J., Joanny J.-F. (2007) Active behavior of the Cytoskeleton. *Phys. Rep* **449**:3-28 <https://doi.org/10.1103/PhysRevLett.78.4510>
38. Prost J., Jülicher F., Joanny J.-F. (2015) Active gel physics. *Nat. Phys* **11**:111-117 <https://doi.org/10.1038/nphys3224>
39. Haertter D., et al. (2024) SarcAsM (Sarcomere Analysis Multi-tool): a comprehensive software tool for structural and functional analysis of sarcomeres in cardiomyocytes.
40. Tiburcy M., et al. (2017) Defined Engineered Human Myocardium With Advanced Maturation for Applications in Heart Failure Modeling and Repair. *Circulation* **135**:1832-1847 <https://doi.org/10.1161/circulationaha.116.024145> | PubMed
41. Harris C. R., et al. (2020) Array programming with NumPy. *Nature* **585**:357-362 <https://doi.org/10.1038/s41586-020-2649-2> | PubMed
42. Virtanen P., et al. (2020) SciPy 1.0: fundamental algorithms for scientific computing in Python. *Nat. Methods* **17**:261-272 <https://doi.org/10.1038/s41592-019-0686-2> | PubMed

Peer reviews

Reviewer #1 (Public review):

Summary:

In this manuscript, the authors present comprehensive experimental observations and a theoretical framework to explain the heterogeneous behaviour of sarcomeres in cardiomyocytes. They show that a stochastic component exists in their contractile activity, which may act as a feedback mechanism regulating physiological function.

Strengths:

Experiments and data analysis are robust and valid. The rigorous statistical analysis and unbiased methods enable the authors to draw well-supported conclusions that go beyond the existing literature. Their outcomes inform about cellular activity at the individual level and the authors explain how the transient dynamics of single sarcomeres are governed by a force-velocity relationship and lead to the complex contractile patterns. The similarity of the results to the study cited in [24] demonstrates the validity of the in vitro setup for answering these questions and the feasibility of such in-vitro systems to extend our knowledge of out-of-equilibrium dynamics in cardiac cells.

Very interesting the suggestion that the interplay between intrinsic fluctuations and the dynamic instability are part of a feedback mechanism for maintaining structural and functional homeostasis.

The addition of the theoretical model and the new text of the manuscript improves the clarity of the study.

<https://doi.org/10.7554/eLife.97321.2.sa3>

Reviewer #2 (Public review):

Summary:

Sarcomeres, the contractile units of skeletal and cardiac muscle, contract in a concerted fashion to power myofibril and thus muscle fiber contraction.

Muscle fiber contraction depends on the stiffness of the elastic substrate of the cell, yet it is not known how this dependence emerges from the collective dynamics of sarcomeres. Here, the authors analyze contraction time series of individual sarcomeres using live imaging of fluorescently labeled cardiomyocytes cultured on elastic substrates of different stiffness. They find that a reduced collective contractility of muscle fibers on unphysiologically stiff substrates is partially explained by a lack of synchronization in the contraction of individual sarcomeres.

This lack of synchronization is at least partially stochastic, consistent with the notion of a tug-of-war between sarcomeres on stiff sarcomeres. A particular irregularity of sarcomere contraction cycles is 'popping', the extension of sarcomeres beyond their rest length. The statistics of 'popping' suggest that this is a purely random process.

Strengths:

This study thus marks an important shift of perspective from whole-cell analysis towards an understanding the collective dynamics of coupled, stochastic sarcomeres.

<https://doi.org/10.7554/eLife.97321.2.sa2>

Reviewer #3 (Public review):

The manuscript of Haertter and coworkers studied the variation of the length of a single sarcomere and the response of microfibrils made by sarcomeres of cardiomyocytes on soft gel substrates of varying stiffness.

The measurements at the level of a single sarcomere are an important new result of this manuscript. They are done by combining the labeling of the sarcomeres z line using genetic manipulation and a sophisticated tracking program using machine learning. This single sarcomere analysis shows strong heterogeneities of the sarcomeres that can show fast oscillations not synchronized with the average behavior of the cell and what the authors call popping events which are large amplitude oscillations. Another important result is the fact that cardiomyocyte contractility decreases with the substrate stiffness, although the properties of single sarcomeres do not seem to depend on substrate stiffness.

The authors suggest that the cardiomyocyte cell behavior is dominated by sarcomere heterogeneity. They show that the heterogeneity between sarcomere is stochastic and that the contribution of static heterogeneity (such as composition differences between sarcomeres) is small.

Strengths:

All the results are, to my knowledge, new and original. The authors also made a theoretical model where each sarcomere is described by a Langevin equation based on a non-linear coupling between force and velocity of the sarcomeres. This model accounts well for the experimental results including the observation of what the authors call popping events.

<https://doi.org/10.7554/eLife.97321.2.sa1>

Author response:

The following is the authors' response to the original reviews.

eLife Assessment

This study provides a valuable characterization of individual sarcomere's contractility and synchrony in spontaneously beating cardiomyocytes as a function of substrate stiffness. The authors, however, provide an incomplete explanation for the observed heterogeneous and stochastic dynamics, so that the work remains mainly descriptive. The work will be of interest to scientists working on muscle biophysics, nonlinear dynamics, and synchronization phenomena in biological systems.

We appreciate the reviewer's insightful comments. A detailed explanation of the described phenomena in the form of a theoretical model and simulations was not included in our manuscript, because we believed it would be most impactful to present a detailed quantitative statistical description of the experiments in one manuscript and then introduce the model, which we already had in preparation, in a separate manuscript to avoid diluting the overall message.

However, following the reviewers' advice, we have now included a comprehensive model into the revised manuscript. This model qualitatively and quantitatively explains the experimentally observed phenomena and introduces a novel class of coupled relaxation oscillators based on a non-monotonic force-velocity relationship of individual sarcomeres. We believe that this addition significantly strengthens the manuscript.

Public Reviews:

Reviewer #1 (Public Review):*Summary:*

In this manuscript, the authors experimentally demonstrated the heterogeneous behavior of sarcomeres in cardiomyocytes and that a stochastic component exists in their contractile activity, which cancels out at the level of myofibrils.

Strengths:

The experiments and data analysis are robust and valid. With very good statistics and unbiased methods, they show cellular activity at the individual level and highlight the heterogeneity between biological networks. The similarity of the results to the study cited in [24] demonstrates the validity of the in vitro setup for answering these questions and the feasibility of such in-vitro systems to extend our knowledge of physiology.

Weaknesses:

Compared to the current literature ([24]), the study does not show a high degree of innovation. It mainly confirms what has been established in the past. The authors complemented the published experiments by developing an in vitro setup with stem cells and by changing the stiffness of the substrate to simulate pathological conditions. However, the experiments they performed do not allow them to explain more than the study in [24], and the conclusions of their study are based on interpretation and speculation about the possible mechanism underlying the observations.

We thank the reviewer for contextualizing our work with the literature. We appreciate the comparison to the study by Kobirumaki-Shimozawa et al. which we cite prominently. They observed stochastically varying beating patterns of individual sarcomeres on a beat-to-beat basis. They propose that this arises from a "titin-based mechanism" operating stochastically, which they interpret as being fundamentally linked to sarcomere-length-dependent effects. This interpretation differs from our model. We feel that the inclusion of our comprehensive model in the revised manuscript will emphasize the significance and novelty of our findings. Our work proposes a distinct alternative mechanistic explanation for the observed stochasticity, grounded in the force-velocity relationship and intrinsic stochasticity, and presents additional novel dynamic phenomena (such as popping and high-frequency oscillations) not reported in the literature yet. We outline the key advancements of our study below:

(1) Physiologically Relevant Human Model System: Our study utilizes human induced pluripotent stem cell-derived cardiomyocytes (hiPSC-CMs). Using a human cell model provides direct relevance for understanding human cardiac physiology and pathophysiology, overcoming limitations inherent in translating findings from rodent models. The hiPSC-CMs exhibit key physiological differences from the mouse ventricular myocytes observed in [24], most notably beating at a significantly lower frequency (~1 Hz or 60 bpm) compared to mice (~5-8 Hz or 300-500 bpm). This difference in timescale is critical as it allowed us to resolve complex intra-beat dynamics that may be different and also harder to observe in mouse cardiomyocytes.

(2) Advanced Experimental Methodology and Resolution: We developed a novel assay incorporating our SarcAsM algorithm for high-throughput tracking and analysis of individual sarcomere dynamics. This approach gave us spatial resolution better than 20 nm at significantly higher sampling rates than previous studies, including Kobirumaki-Shimozawa et al. Furthermore, our high-throughput *in vitro* approach made it possible to analyze vastly larger datasets than, e.g., the study by Kobirumaki-Shimozawa et al. (which reports observations from fewer than 20 myofibrils, encompassing less than 200 sarcomeres in total).

While we recognize that *in-vivo* tissue studies present unique experimental challenges, the substantially greater statistical power of our study is crucial for reliably characterizing the complex, stochastic dynamics we report. The enhanced resolution and statistical robustness are not merely incremental; they enable the detailed identification and analysis of heterogeneous behaviors that were previously inaccessible or could not be characterized with the same level of confidence.

(3) Novel Observed Phenomena: Our high-resolution data reveals specific dynamic behaviors, such as sarcomere "popping" and high-frequency oscillations during contraction, which, to our knowledge, have not been previously reported or characterized in cardiomyocytes. The resolution limitations and the high beating frequency in mouse models may not have permitted the observation of these subtle, but potentially important phenomena.

(4) Distinct Mechanistic Explanation and Model: Kobirumaki-Shimozawa et al. propose a qualitative model where sarcomere motion variability primarily arises from length-dependent activation. This view is essentially a static one, based on a long history of isometric skeletal muscle experiments, where time-dependent forces are not relevant. We argue that in highly dynamic cardiomyocytes this may not be the most useful approach. While we acknowledge length dependence can play a role, our integrated experimental-theoretical work proposes a different primary mechanism. Our model demonstrates that the observed stochastic heterogeneity and beat-to-beat variations, including the oscillatory motion and popping, can be quantitatively explained by dynamic instabilities arising from a non-monotonic force-velocity relationship of individual sarcomeres in conjunction with intrinsic sarcomere-level stochastic fluctuations. The model emphasizes the active, transient nature of force generation rather than solely assuming length dependence. Our model provides an alternative explanation for the observed dynamics, and a quantitative, mechanism-based understanding.

Reviewer #2 (Public Review):

Summary:

Sarcomeres, the contractile units of skeletal and cardiac muscle, contract in a concerted fashion to power myofibril and thus muscle fiber contraction.

Muscle fiber contraction depends on the stiffness of the elastic substrate of the cell, yet it is not known how this dependence emerges from the collective dynamics of sarcomeres. Here, the authors analyze the contraction time series of individual sarcomeres using live imaging of fluorescently labeled cardiomyocytes cultured on elastic substrates of different stiffness. They find that reduced collective contractility of muscle fibers on unphysiologically stiff substrates is partially explained by a lack of synchronization in the contraction of individual sarcomeres.

This lack of synchronization is at least partially stochastic, consistent with the notion of a tug-of-war between sarcomeres on stiff sarcomeres. A particular irregularity of sarcomere contraction cycles is 'popping', the extension of sarcomeres beyond their rest length. The statistics of 'popping' suggest that this is a purely random process.

Strengths:

This study thus marks an important shift of perspective from whole-cell analysis towards an understanding of the collective dynamics of coupled, stochastic sarcomeres.

Weaknesses:

Further insight into mechanisms could be provided by additional analyses and/or comparisons to mathematical models.

We thank the reviewer for the feedback. We have enhanced the manuscript by a comprehensive dynamic model, that we also contrast with previously proposed models.

Reviewer #3 (Public Review):

Summary:

The manuscript of Haertter and coworkers studied the variation of length of a single sarcomere and the response of microfibrils made by sarcomeres of cardiomyocytes on soft gel substrates of varying stiffnesses.

The measurements at the level of a single sarcomere are an important new result of this manuscript. They are done by combining the labeling of the sarcomeres z line using genetic manipulation and a sophisticated tracking program using machine learning. This single sarcomere analysis shows strong heterogeneities of the sarcomeres that can show fast oscillations not synchronized with the average behavior of the cell and what the authors call popping events which are large amplitude oscillations. Another important result is the fact that cardiomyocyte contractility decreases with the substrate stiffness although the properties of single sarcomeres do not seem to depend on substrate stiffness.

The authors suggest that the cardiomyocyte cell behavior is dominated by sarcomere heterogeneity. They show that the heterogeneity between sarcomeres is stochastic and that the contribution of static heterogeneity (such as composition differences between sarcomeres) is small.

Strengths:

All the results are to my knowledge new and original and deserve attention.

Weaknesses:

However, I find the manuscript a bit frustrating because the authors only give very qualitative explanations of the phenomena that they observe. They mention that popping could be explained by a nonlinear force-velocity relation of the sarcomere leading to a rapid detachment of all motors. However, they do not explicitly provide a theoretical description. How would the popping depend on the parameters and in particular on the substrate stiffness? Would the popping statistics be affected by the stiffness? It is also not clear to me how the dependence on the soft gel stiffness of the cardiomyocyte cell can be explained by the stochasticity of the sarcomere properties. Can any of the results found by the authors be explained by existing theories of cardiomyocytes? The only one I know is that of Safran and coworkers.

I also found the paper very difficult to read. The authors should perhaps reorganize the structure of the presentation in order to highlight what the new and important results are.

We are grateful for this detailed and critical feedback. The observed phenomena (stochastic heterogeneity, popping, high-frequency oscillatory motion) can indeed be explained by a nonmonotonic force-velocity relation along with stochastic fluctuations of individual sarcomeres. At the time of initial submission of this manuscript, we already had a theoretical model in preparation, which both qualitatively and quantitatively explains the observed phenomena. As a result, we included certain interpretations preemptively, which caused some lack of clarity in the absence of the full model. We have now added the model to this manuscript, providing a mechanistic interpretation of our findings. The model is different from prior models in that it emphasizes time-dependent forces, typically disregarded in models built to understand isometric skeletal muscle experiments.

We have shortened, streamlined and restructured our manuscript to improve the readability and accessibility of our study.

Recommendations for the authors:

There is a consensus among reviewers that the link between the stiffness dependence of the observed stochastic dynamics and the proposed tug-of-war mechanism is unclear. More quantitative support and discussion is required, possibly using theoretical modeling.

We are grateful for the insightful and comprehensive feedback by both editor and reviewers. As suggested, we have now added a comprehensive model explaining the observed phenomena and presenting a new conceptual view on cardiac muscle dynamics.

Reviewer #1 (Recommendations For The Authors):

The authors addressed an interesting question related to the dynamics of cardiac cells and their multiscale dynamics. They did a good job in terms of experimental design and data analysis. However, I fear that they do not contribute enough new information to the topic.

The authors should refer to the study in [24] and explain better the difference between these two studies. Although the different approaches are quite obvious, it is not clear to me what additional insights they add to the problem. They conducted their experiments with different stiffnesses. However, the conclusions they draw from the study are based on speculation (e.g. about the behavior of myosin heads in relation to shortening and relaxation), while their data mainly confirm previous studies. They need to address more explicitly the novelty of their study.

Novelty and Comparison with Previous Studies: We understand the concern about distinguishing our contribution from prior work, specifically Kobirumaki-Shimozawa et al., 2021.

As detailed in our public response, these are the key advances:

Use of a medically relevant human iPSC-CM model vs. mouse cardiomyocytes.

Superior spatial and temporal resolution via our SarcAsM algorithm, revealing novel phenomena like popping and high-frequency oscillations not previously reported.

Significantly greater statistical power due to our high-throughput *in vitro* assay.

We added a distinct mechanistic explanation based on the dynamic force-velocity relationship and sarcomere-level stochasticity, contrasting with the static, deterministic titin/length-dependence focus of previous studies.

Interpretation and Speculation: We acknowledge that without the explicit model, some interpretations in the initial submission appeared speculative. As noted in our public response, we had already started to develop a theoretical model explaining our observations at the time of submission, targeting a second follow-up publication. Including interpretations based on this unpublished model prematurely clearly caused confusion. We now include the full model in the revised manuscript.

Integration of the Theoretical Model: We have now fully integrated the model into the revised manuscript. The model explicitly demonstrates how the non-monotonic force-velocity relationship of individual sarcomeres leads to dynamic instabilities around a critical force threshold. This instability along with stochasticity drives a 'tug-of-war' between coupled sarcomeres, generating complex emergent behaviors.

Mechanistic Explanation Beyond Length-Dependence: Our model quantitatively reproduces all key experimental findings (stochastic heterogeneity, popping, oscillations) without relying on length-dependent activation effects. This strongly supports our conclusion that the active, transient dynamics of individual sarcomeres governed by the force-velocity relationship are fundamental drivers of these complex contractile patterns. We believe this provides a significant conceptual advance, highlighting a potentially underappreciated aspect of sarcomere dynamics. Previous models focused mostly on length-dependence, historically based on skeletal muscle fiber experiments that were often done under static, isometric conditions. We feel that the new model represents a substantial paradigm shift in understanding highly dynamic muscles such as heart muscle.

We are confident that the inclusion of the model addresses the majority of the reviewer's concerns.

Additional comments:

The authors write of a tug-of-war competition between the sarcomeres, and I'm not sure what they mean by that. I would spend more words explaining this point, especially because it seems to be an important point to describe their results. Similarly, they talked about an all-or-nothing phenomenon when they described the elongation of sarcomeres. What do they mean by this?

We have revised the manuscript where clarification was needed and now define the terms mentioned more explicitly.

(1) "Tug-of-War": We used this term metaphorically to describe the mechanical competition between linearly coupled sarcomeres within a myofibril, especially when contracting against rigid external boundary conditions. While it is not a perfect analogy, the metaphor intuitively captures the inherent instability of this interaction: similar to how a team in a real tug-of-war might suddenly yield when one person tires and the rest of team gets overloaded, rather than steadily losing ground, the dynamic instability arising from the non-monotonic force-velocity relationship (detailed in our model, lines 300ff) can cause individual sarcomeres to abruptly change state (e.g., shorten or rapidly lengthen) while under tension from their neighbors. We have removed the term from the title and now use it more sparingly within the manuscript to better reflect its role as an illustrative analogy.

(2) "All-or-Nothing" Elongation (Popping): The term "popping" describes our experimental observation of sudden, rapid, and extensive elongation of individual sarcomeres. This typically occurs late in the contraction cycle during early relaxation, when overall force may be declining, but individual sarcomeres can still experience significant tension from their neighbors. We described this specific type of rapid elongation in the original manuscript as an "all-or-nothing" phenomenon because, typically, sarcomeres in these events yield rapidly and strongly overshoot their resting length without recovering in a given activation cycle.

The speed of popping events is substantially higher than the speed of coordinated gradual shortening observed during systoles that is driven by bound myosin heads. This observation strongly suggests an instability-driven, avalanche-like unbinding of myosin heads from the actin filaments during these events.

We agree that the term "all-or-nothing" is not precise, and we have removed it, as it is not essential for describing the observed "popping" dynamics.

The authors claim that the popping frequency increases as a function of stiffness. However, Figure 4E does not really seem to be a common practice in terms of statistical significance. A better description could help to remove this doubt.

We clarified the presentation of popping frequency data and its statistical interpretation.

(1) Popping Frequency vs. Substrate Stiffness (previously Figure 4D, now Figure 3G):

We first corrected that the dependence of popping frequency on substrate stiffness was presented in Figure 4D, not 4E. In the revised, shortened manuscript it can be now found in Fig. 3G. Due to the large number of observations (N) in our dataset, the slight upward trend in popping frequency with increasing substrate stiffness shown in Figure 4D does reach statistical significance using standard tests. For details see Figure captions.

(2) Popping Frequency vs. Sarcomere Resting Length (previously Figure 4E, now Figure 3H):

Figure 4E addresses the relationship between popping frequency and the individual sarcomere's resting length. To generate this plot, we binned sarcomeres based on their measured resting length (in intervals of 0.02 μm) and calculated the mean popping frequency within each bin across all conditions. We have now clarified this in the figure caption.

(3) Interpretation of Length Dependence:

While Figure 3H clearly shows that longer sarcomeres are more prone to popping, we argue this is likely a modulating factor rather than the sole underlying cause. Two key observations support this interpretation:

Even very short sarcomeres (e.g., < 1.65 μm resting length) exhibit a non-zero popping frequency (around 5-10%), indicating that popping is not exclusive to long sarcomeres.

The distribution of resting lengths, now added to the graph, is narrower than the wide range (1.6-2.0 μm) plotted in Figure 3H. Popping still occurs stochastically within a myofibril of sarcomere with relatively similar resting lengths.

Therefore, while length clearly influences the probability of popping, the phenomenon itself appears to be fundamentally stochastic, occurring across a range of lengths. This is consistent with our model in which dynamic instabilities (driven by the non-linear force-velocity relationship) and stochastic fluctuations are the primary triggers, while length affects probability of occurrence.

Changes in Manuscript:

We have revised the text associated with Figures 3G and 3H to clarify the distinction between stiffness and length dependence.

We have added a statement in the Methods section and figure legends (e.g., Legend for Fig 3) explaining our approach to statistical analysis and interpretation for large datasets where standard p-values may be less informative.

We believe these clarifications directly address the reviewer's concerns about the data presentation and interpretation in Figure 3.

Reviewer #2 (Recommendations For The Authors):

This is an interesting study, which however could and should be extended, see below. The current manuscript contains much less information than its length suggests; its figures contain partially redundant data.

Taking into account this critical feedback, we have restructured, streamlined and shortened the manuscript to improve readability and accessibility.

(1) How regular are the cellular contraction cycles?

Have the authors computed a coefficient of variation of cycle durations?

Does this regularity depend on substrate stiffness?

We have substantially improved the detection accuracy of contraction intervals compared to our initial submission (details see SarcAsM, <https://www.biorxiv.org/content/10.1101/2025.04.29.650605v1> [↗](#)). We calculated the beating rate variability (defined as the standard deviation of cycle durations), and found a low variability of on average less than 0.05 s across the tested conditions. The distribution of this variability is positively skewed, with the majority of values clustering near zero. We have added new panels showing these results to Fig. S2B.

(2) Which experiments could the authors perform to identify the origin of the apparent 3-Hz oscillations?

Would these oscillations persist even if the cardiomyocytes would not beat?

We now address these questions in the revised manuscript.

(1) Active Nature: The ~3 Hz oscillations are clearly linked to active contraction. They are absent in quiescent, non-beating cardiomyocytes observed under identical conditions, confirming that they are not passive fluctuations or baseline cellular tremors.

(2) Signal Fidelity: We are confident these are genuine physiological events, not artifacts. Our high temporal resolution (~15 ms frame time) and tracking accuracy (< 20 nm) allow reliable detection because events are well above system noise. This is now explained in the revised manuscript.

(3) Can the authors augment their study by modeling?

For example, could the experimental data be fitted by a Kuramoto-type model of the form $d\phi_i/dt = \epsilon \sin(\Omega - \phi_i) + \lambda \sin(\phi_i - \phi_{i+1}) + \xi_i$, combining phase-locking of sarcomere oscillations with phase ϕ_i to intracellular calcium oscillations with phase Ω , and anti-phase synchronization between neighboring sarcomeres, as well as noise ξ_i ?

If yes, how would the coupling strength depend on substrate stiffness?

We now added a model. While a Kuramoto-type phase model is powerful for studying synchronization, we determined that a more mechanistic approach was required. Crucially, sarcomeres are mechanically coupled in series within a myofibril, and this direct physical linkage is not well-represented by the abstract, phase-based coupling of a Kuramoto model.

Instead, our model comprises serially coupled sarcomeres, each governed by an underdamped Langevin equation. This framework allowed us to infer the force-velocity relation without any prior assumptions directly from our experimental data, revealing a critical non-monotonic characteristic. As we now emphasize in the revised manuscript, this

behavior is mathematically equivalent to a Van-der-Pol relaxation oscillator, which reflects the instability-driven nature of the system.

Furthermore, and in line with the reviewer's suggestion, our model incorporates a stochastic noise term which we found essential for reproducing the observed phenomena. Without this noise term, the characteristic sarcomere dynamics do not emerge (Fig. 5).


(4) What is the maximally extended length of titin, and how does this length correspond to the maximal length of popping sarcomeres?

The force-extension curves of titin have been measured in single-molecule experiments (and the packing density of titin is known) - can the authors use this information to infer the forces acting inside sarcomeres?

We thank the reviewer for this thoughtful question. While sarcomere length during popping can be measured, inferring the corresponding intra-sarcomeric force is not straightforward in a living, contracting cardiomyocyte. The relationship between extension and force is complex and dynamic, involving multiple molecular components.

Our data show elongations up to 0.5 μm during popping events. While this magnitude is plausibly within the extensibility range of titin and other mechanically relevant components (Caporizzo & Prosser, 2021; Loescher & Linke, 2023), directly inferring force from this observation is challenging. In such a multi-component system with both active and passive elements, total force comprises several factors that cannot be disentangled from a simple length measurement alone. First, the system is dominated by active, velocity-dependent force generation of cross-bridges, which our model shows is non-monotonic. Second, titin exhibits a restoring force that is strongly strain-rate dependent (Rief et al., 1997), critical during rapid elongation. Third, viscous drag forces within the sarcomere are also highly strain-rate dependent, contributing significantly during rapid length changes. Fourth, other structural elements such as microtubules and intermediate filaments contribute to viscoelastic properties, particularly at high strains (Caporizzo & Prosser, 2021). This complex interplay makes it impossible to map a given sarcomere length to a unique force value using single-molecule titin data alone.

(5) I urge the authors to make their raw data openly available.

We agree on the importance of data availability. While the complete raw imaging dataset is several hundred gigabytes and thus impractical to deposit, we have uploaded a comprehensive dataset to Zenodo to ensure full reproducibility. This repository includes a representative subset of raw imaging data (50 cells per condition), with corresponding sarcomere motion data provided in a readable JSON format. Crucially, the deposition also contains the complete aggregated data underlying all figures and statistical analyses presented in the manuscript. All provided data can be programmatically accessed and analyzed using our SarcAsM Python API. The data can be accessed at: <https://doi.org/10.5281/zenodo.17564384> .

Minor

(1) How did the authors determine the start and end of contraction cycles when analyzing their data?

The start and end points of each contraction cycle were identified using ContractionNet, a custom convolutional neural network we developed for this purpose. This method, used for all analyses in the revised manuscript, detects contraction intervals with high accuracy directly from sarcomere dynamics time-series data and significantly outperforms the threshold-based approach used previously. The complete methodology, algorithm description,

and validation of ContractionNet are detailed in our companion paper on the SarcAsM analysis software

(www.biorxiv.org/content/10.1101/2025.04.29.650605v1 [↗](#), see Fig. S6).

| (2) *What are the measurement errors in determining Delta_SL?*

The measurement error for the Z-band trajectories is approximately 17 nm. This high tracking accuracy is achieved with our deep-learning-based Z-band segmentation approach, which employs a 3D convolutional neural network (3D U-Net) to leverage both spatial and temporal context for robust Z-band segmentation in noisy, high-speed recordings. A full description of this validation is available in our SarcAsM companion paper (see Figure S3 therein).

| (3) *Does popping occur while other sarcomeres are still contracting?*

This is an important point. Yes, popping frequently occurs while other sarcomeres within the same myofibril are still actively shortening. This simultaneity is clearly visualized in the newly added Movie M1, which displays a phase-space plot (velocity vs. length change relative to rest) for all tracked sarcomeres over time. In this visualization, popping events appear as trajectories moving into the top-right quadrant (rapid elongation), while concurrently, other sarcomeres are represented by points in the left quadrants (negative velocity), indicating ongoing shortening. We have included Movie M1 as supplementary material.

| (4) *The authors argue that their data on popping sarcomeres is consistent with homogeneous popping probabilities.*

| (5) *Can the authors assess in simulations how dispersed the popping probabilities of individual sarcomeres could be before they would notice a statistically significant difference to the homogeneous case?*

This question touches on a key challenge in analyzing these complex dynamics. A direct statistical test of popping probability for each individual sarcomere is not feasible, as the number of events per sarcomere over our observation time is too low for robust single-unit analysis. Consequently, our approach relies on testing the cumulative distributions of inter-event spatial distances and temporal gaps across all sarcomeres within a given region (LOI).

In nearly half of the analyzed LOIs, these cumulative distributions were statistically indistinguishable ($p > 0.05$) from the geometric distribution expected for a single, homogeneous stochastic process. This provides strong support for our primary conclusion that popping is fundamentally a random phenomenon.

For the cases that deviate from the homogeneous model, we argue that this does not refute the underlying stochasticity of the events. Instead, we propose this is the expected statistical signature of pooling data from a population of sarcomeres that have slight, intrinsic variations in their individual popping probabilities due to factors like resting length or structural integrity. Even if each sarcomere's popping is a locally random event, a cumulative test performed on a population with varied baseline probabilities is expected to detect a deviation from a simple, homogeneous model.

Regarding the requested simulation study: While we agree this would be methodologically informative, the sensitivity to detect probability dispersion depends on multiple interacting factors (number of sarcomeres per LOI, observation time, event rates, and the assumed form of heterogeneity). Any single simulation scenario would therefore be highly model-dependent and of limited generality. Rather than introducing additional assumptions, we base our conclusions on the observed agreement with the homogeneous model in approximately half of LOIs and the correlation of deviations with measurable properties (Fig. 4E). A

comprehensive statistical analysis would constitute a substantial methodological study beyond the scope of this mechanistically focused manuscript.

(6) Can the authors measure sarcomere rest length and check if this rest length is correlated with the popping probability of individual sarcomeres?

Yes, we performed this analysis. As shown in Figure 3H (previously Fig. 4E), we found a positive correlation between sarcomere resting length and popping frequency, confirming that longer sarcomeres have a higher probability of popping.

Importantly, however, the popping probability remains non-zero even for shorter sarcomeres. As detailed in our response to Reviewer #1 regarding this figure, we interpret resting length as a significant modulating factor that influences popping probability, rather than the sole determinant of the phenomenon.

(7) Several mathematical models of sarcomere contraction exist (e.g., crossbridge models).

(8) Could the authors perform computer simulations of several such stochastic sarcomere models coupled in series?

Alternatively, could the authors discuss this?

As I understand, references 16-18 model myofibril contraction assuming static variability of sarcomeres, but do not account for stochasticity in the contractility of individual sarcomeres.

We thank the reviewer for this excellent suggestion. We have performed such simulations, and the theoretical model is a central component of our revised manuscript (new Figures 4 and 5; manuscript lines 316ff).

As the reviewer points out, previous models (e.g., refs 12 and 14 in our manuscript) have often relied on predefined static variability between sarcomeres to explain heterogeneous behavior. Our work takes a fundamentally different approach. We model the myofibril as a chain of serially coupled sarcomeres, where the dynamics of each unit are governed by an underdamped Langevin equation. This formulation inherently incorporates stochasticity and describes the interplay between a non-monotonic, velocity-dependent active force, a length-dependent passive force, and the mechanical coupling to its neighbors.

Crucially, the model parameters were not assumed, but were instead inferred by fitting the model directly to our experimental data using a gradient-free optimization algorithm. This data-driven stochastic model was sufficient to quantitatively reproduce key observed phenomena, including high-frequency oscillations and popping events. Our central finding is that these complex behaviors emerge naturally from the coupled system, driven by the non-monotonic force-velocity relationship and intrinsic stochastic fluctuations. This demonstrates that predefined static heterogeneity is not required to explain the observed dynamics.

(9) The manuscript could be shortened (e.g., lines 52-56 in the introduction provide little extra value).

We have significantly revised the entire manuscript to improve clarity and readability. We have removed sentences in the introduction as suggested and substantially restructured major sections. One of the main reasons for this was the integration of our theoretical model, which was originally prepared as a separate manuscript. This required us to completely reframe the introduction and reorganize the figures and results.

We are confident that these extensive changes have resulted in a stronger, more concise and impactful paper that now integrates our experimental findings with a theoretical model.

(10) Figure 2 is overloaded with data. Several panels could be moved to the SM without compromising the key message.

Introducing the notation in panels Figures 2A-C does not seem ideal to me; maybe add a cartoon?

We agree that the Fig. 2 was dense. We have redesigned panels A-F to improve clarity and better guide the reader. We now use a consistent color-coding scheme to link the extrema in the phase portraits (A-C) to the corresponding distributions of individual sarcomeres (E-G). We have also revised the accompanying text to make the figure's logic more transparent.

We have considered moving panels A-C to the supplementary materials. However, we believe their placement in the main text is crucial for two reasons:

(1) Revealing Core Dynamics: The length-velocity phase portrait is the first visualization that reveals the underlying near-oscillatory dynamics of individual sarcomeres. This was not an assumed behavior but a critical experimental observation that directly motivated our entire theoretical modeling effort. We now also provide animated versions of these plots (Movies X-Y) to further illustrate these complex dynamics.

(2) Enabling Model-Experiment Comparison: A phase portrait is a standard tool for comparing experimental data with theoretical models. Retaining it in the main text allows us to directly compare data and model in our new Figures 4 and 5, providing a clear validation of our model.

(11) Similarly, Figures 4F, G, and H seem dispensable to me.

(I also wonder how clear the analogy of a coin flip is if a biased coin with probabilities p and $1-p$ needs to be used.)

We agree that the previous Figure 4F, which served a purely illustrative purpose, was dispensable and have removed it. The "coin flip" analogy was potentially confusing and we have removed it.

As part of a broader restructuring of the manuscript, the quantitative analyses from the original Figures 4G and 4H are now presented as Figures 3I and 3J. They provide important supporting evidence for the stochastic nature of the resulting popping events. We believe retaining this quantitative analysis is valuable, and we hope that by streamlining the figure and removing the analogy, we have addressed the reviewer's concerns.

(12) Equation (1) is unnecessarily complicated. The same holds for Equation (2).

It might make sense to separate definitions for serial and mutual correlations.

(This would also simplify the axes labels in Figure 3C.)

(13) The notation used in Equation (1) is not fully clear.

I assume t denotes a unit-less time index and T is the unit-less duration of a contraction cycle, measured in multiples of a fixed time interval?

Regarding comments (12) and (13):

We thank the reviewer for these helpful suggestions. In response to comment (12), we have separated the definitions for the mutual (r_m) and serial (r_s) correlation coefficients, presenting them as distinct calculations rather than as special cases of a single, more complex formula. This makes their definitions more direct and explicit. The calculation for the serial correlation coefficient has also been streamlined into a concise inline definition.

In response to comment (13), we have clarified the notation in Equation (1). In the manuscript text (lines 208f), we now explicitly state that t represents the discrete, unitless time index (i.e., the frame number) within a time-series, and T is the total number of frames (i.e., the total duration in frames) of a given contraction cycle.

While Equation (1) itself is the standard definition for the uncentered correlation coefficient and cannot be algebraically simplified, we have added text to specify this and justify its use. This metric (equivalent to cosine similarity) is appropriate for our analysis as it assesses the similarity in the shape of motion patterns, independent of their mean values.

Finally, to further streamline the paper, we have removed the velocity correlation analysis and the corresponding parts of Figure 3.

(14) The authors should make clear in all figures what is experiment and what is simulation.

We have now clarified the nature of each graph in the figure captions.

(15) The caption of Figure 3C could be simplified.

We have simplified all figure captions.

(16) I found Figure 3A hard to understand.

We concluded that Figure 3A was confusing and did not add essential information to the manuscript. We have removed it entirely.

Reviewer #3 (Recommendations For The Authors):

In conclusion, I think that the manuscript would gain a lot if some more precise and more quantitative interpretation of the results were given. This might require a collaboration with theorists.

We have integrated a novel theoretical framework into the revised manuscript (new Figures 4 and 5; manuscript lines 300ff as described above).

This new section introduces a data-driven, stochastic dynamical model that simulates the myofibril as a chain of serially coupled sarcomeres. Each sarcomere's motion is governed by an underdamped Langevin equation, a formulation that inherently accounts for stochasticity. Crucially, our model incorporates a non-monotonic force-velocity relationship inferred directly from our experimental data, rather than relying on predefined static variability between sarcomeres a key distinction from previous theoretical work.

This integrated model successfully and quantitatively reproduces all major experimental phenomena described in the paper, including high-frequency oscillations and stochastic "popping" events. It demonstrates that these complex behaviors emerge naturally as dynamic instabilities from the coupled system. This addition elevates the manuscript from a descriptive study to one that provides a predictive, mechanism-driven framework for understanding sarcomere dynamics.

<https://doi.org/10.7554/eLife.97321.2.sa0>